# Feasible Path Synthesis for Automated Guided Vehicles

Reijer Idema

2005


TU Delft
Julianalaan 134
2628 BL Delft


FROG Navigation Systems
Krommewetering 21
3543 AP Utrecht

# Feasible Path Synthesis for Automated Guided Vehicles

*Author:*
Reijer Idema

*Supervisors:*
prof.dr.ir. P. Wesseling *(TU Delft)*
dr.ir. Kees Vuik *(TU Delft)*
ir. Patrick H.F. Segeren *(FROG)*
dr.ir. René Jager *(FROG)*

December 12, 2005

# Preface

This is a research report for the degree of Master of Science for the study Applied Mathematics, faculty of Electrical Engineering, Mathematics and Computer Science of the Delft University of Technology. The graduation work was done in the unit of Numerical Analysis, taking a total of nine months of work.

The first three months focused on problem definition, study of literature, and planning the research for the next six months. The work done in this period is reported in [Ide05]. The remaining six months of the graduation work were spend on the actual research of finding a solution for the defined problem. Of that second period this is the report.

The research project was carried out at FROG Navigation Systems. FROG is a manufacturer of Automated Guided Vehicles. They have developed a multitude of vehicles that transport products within factories of companies like Sony and General Motors, but also have an automatically driven bus for public transport driving in the center of Eindhoven. For more information see their website `www.frog.nl`.

# Contents

# 1 Introduction

In the preceding preliminary research report [Ide05], we introduced the following general problem description.

*Suppose an AGV has to perform an action in the world.*
*Find the best control input for the AGV to achieve the action.* (1)

We have shown that for our application we could split all actions, that are not related to the path the vehicle drives, out of the problem. Thus we focused on the task of finding a path between two points.

Within this task we distinguished four stages.

**Internal constraint research:** research into the constraints on a path as a result of the limitations of the vehicle control mechanism, e.g., maximum speed and minimum radius needed to be able to take a corner.

**External constraint research:** research into the constraints on a path as a result of the dimensions of the vehicle and obstacles along the path, but also things like speed restrictions for a certain road.

**Cost and heuristics research:** research to uncover how to quantify if a path is good or bad, and to find heuristics to find a good path.

**Solver algorithm research:** when the first three stages of research are finished, the results can be used in a solver algorithm to automatically find a good path. The final stage is to investigate what solver algorithm is best suited for that task.

This research report focusses mainly on the first stage, the internal constraint research, focusing on the geometrical aspects of vehicle paths.

We start with the introduction of a general definition of the vehicle path concept in Section 2, and define some important operations on vehicle paths. Followed by the introduction of the vehicle model we will use in Section 3, and a treatment of the limitations of the steering mechanism with the resulting restrictions on a vehicle path. As we will show, these restrictions can be expressed in the curvature of the path curve and its derivative.

As was explained in the preceding preliminary research report, the mathematical representation of choice for vehicle paths is that of B-Splines and NURBS. In Section 4 we start to use B-Splines as a mathematical description for a vehicle path. Further we introduce control point repositioning on B-Splines. This is the operation that we are using to change the shape of a path curve throughout this report.

Then in Section 5 we combine the work of the preceding sections into the feasible repositioning set concept. These are sets of all control point repositionings on a path that change the path into one that satisfies the path restrictions treated in Section 3. We show how to calculate such sets, not only giving us a method to check if a path meets the restrictions, but also handing us a tool to find a feasible path in a smart way.

Next, in Section 6 we extend the notion of control point repositioning. We show that the results of Section 5 are also usable on NURBS curves, and that we can reposition multiple control points at once instead of the single control points repositioning we originally focused on.

The next step is to develop a method to construct vehicle paths. There are many ways to do this. Our method of choice is treated in Section 7. We show how to create single bend curves, and how to merge them together into a larger path curve. Further we show how to use the results of the preceding sections to guarantee that the path we construct can actually be driven by the vehicle for which it is designed.

Finally, in Section 8 we reflect on the entire research project, and make some recommendations for further research.

# 2 Vehicle Paths

This section introduces the general definition of a vehicle path, and treats some basic operations on vehicle paths. These operations are calculating the distance the vehicle traveled, calculating the speed of the vehicle, and calculating the curvature of the path.

**Definition 2.1.** *A vehicle path is a continuously differentiable curve*

$$\mathbf{C}(u) = \begin{pmatrix} x(u) \\ y(u) \end{pmatrix} , \quad u \in [a,b] ,$$

*with*

$$\left|\left|\mathbf{C}'(u)\right|\right|_2 \neq 0 , \quad u \in [a,b] .$$

*We call* $\mathbf{C}(a)$ *the start point, and* $\mathbf{C}(b)$ *the endpoint of the path.*

The above definition specifies a geometric curve parameterized by $u$. This does not specify, however, where the vehicle is at a certain time $t$. So a vehicle path alone is not enough to specify how a vehicle should drive from the start point to the endpoint. To accomplish a full specification we use a time-parameter function, that defines which parameter value $u$ belongs to a certain time $t$.

**Definition 2.2.** *A time-parameter function is a continuously differentiable function*

$$u_T(t) , \quad t \in [t_a, t_b] ,$$

*such that*

$$\begin{aligned} u_T(t_a) &= a , \\ u_T(t_b) &= b , \\ u_T'(t) &> 0 , \quad t \in (t_a, t_b) . \end{aligned}$$

Note that the positivity requirement $u_T'(t) > 0$ for all $t \in (t_a, t_b)$, together with $u_T(t)$ being continuously differentiable, makes that

$$u_T'(t) \geq 0 , \text{ for all } t \in [t_a, t_b] .$$

The time-parameter function $u_T(t)$ should be interpreted as a reparameterization function for $\mathbf{C}(u)$, such that $\mathbf{C}(u_T(t))$ is the position of the vehicle at time $t$. The vehicle is not allowed to stop along its path, except in the start point or endpoint, neither is the vehicle allowed to drive backwards. These restrictions are ensured by the positivity requirement on $u_T'(t)$. Stopping and reverse gear operations should be implemented by using multiple contiguous vehicle paths.

In this section we introduce definitions for the distance traveled over a vehicle path, the velocity of the vehicle and the curvature at a point on the path. These quantities should reflect the actual situation of a vehicle driving along the path, therefore they should all be defined with respect to the time $t$.

However in practice, the time-parameter function $u_T(t)$ is usually not known explicitly. It is only implicitly defined by a speed function for the vehicle. We would like to do as much operations and calculations on the vehicle path as possible, before defining that speed function. For example, we would like operations on the vehicle path that ensure that a physical vehicle can actually follow it, and that the vehicle can drive the path as fast as possible. Obviously these operations should be executed before a speed function for the vehicle is chosen.

Therefore we also provide definitions of the above mentioned quantities, that depend on the curve parameter $u$. Quantities and operations that can be fully defined without the use of the time $t$ we call static. Quantities and operations that need the use of the time $t$ we call dynamic.

## 2.1 Distance

The distance is the arc length of a certain part of the vehicle path. This is a geometric quantity and should therefore be independent of the time-parameter function. We use the formula for the arc length to define the distance, both with respect to the time $t$ and with respect to the curve parameter $u$. Then we prove that these definitions are indeed consistent with each other.

**Definition 2.3.** *Let $\mathbf{C}(u_T(t))$ be a continuously differentiable vehicle path. Then the distance $s_T(t)$ from the start point to $\mathbf{C}(u_T(t))$ is*

$$s_T(t) = \int_{t_a}^{t} \left\| \frac{d\mathbf{C}}{dt}(u_T(\tau)) \right\|_2 d\tau\,, \quad t \in [t_a, t_b]\,.$$

*Let $\mathbf{C}(u)$ be a continuously differentiable vehicle path. Then the distance $s(u)$ from the start point to $\mathbf{C}(u)$ is*

$$s(u) = \int_{a}^{u} \left\| \frac{d\mathbf{C}}{du}(\mu) \right\|_2 d\mu\,, \quad u \in [a, b]\,.$$

**Theorem 2.1.** *The definitions of $s_T(t)$ and $s(u)$ are consistent with each other, i.e.,*

$$s_T(t) = s(u_T(t))\,.$$

*So the distance is a static quantity.*

*Proof.* Using that $u_T'(t)$ is nonnegative we can write

$$\begin{aligned} s_T(t) &= \int_{t_a}^{t} \left|\left| \frac{d\mathbf{C}}{dt}(u_T(\tau)) \right|\right|_2 d\tau \\ &= \int_{t_a}^{t} \left|\left| \frac{d\mathbf{C}}{du}(u_T(\tau))\, u_T'(\tau) \right|\right|_2 d\tau \\ &= \int_{t_a}^{t} \left|\left| \frac{d\mathbf{C}}{du}(u_T(\tau)) \right|\right|_2 u_T'(\tau)\, d\tau \\ &= \int_{t_a}^{u_T(t)} \left|\left| \frac{d\mathbf{C}}{du}(\mu) \right|\right|_2 d\mu \quad = \quad s(u_T(t)) . \end{aligned}$$

□

## 2.2 Velocity

The velocity is the speed with which the vehicle traverses the path, with respect to time. This is obviously a dynamic quantity.

**Definition 2.4.** *Let $\mathbf{C}(u_T(t))$ be a continuously differentiable vehicle path. Then the velocity $v_T(t)$ of the vehicle at time $t$ is*

$$v_T(t) = \frac{ds_T}{dt}(t) = \left|\left| \frac{d\mathbf{C}}{du}(u_T(t)) \right|\right|_2 u_T'(t) , \quad t \in [t_a, t_b] .$$

*Let $\mathbf{C}(u)$ be a continuously differentiable vehicle path. Then the velocity $v(u)$ of the vehicle at parameter value $u$ is*

$$v(u) = v_T(t_u) , \quad u \in [a, b] ,$$

*where $t_u$ is such that $u_T(t_u) = u$.*

This is where we use the requirement $||\mathbf{C}'(u)||_2 \neq 0$ imposed on a vehicle path in Definition 2.1. Suppose that $||\mathbf{C}'(\tilde{u})||_2 = 0$ for some $\tilde{u} \in [a, b]$, and let $\tilde{t}$ be such that $u_T(\tilde{t}) = \tilde{u}$, then

$$v_T(\tilde{t}) = \left|\left|\mathbf{C}'(\tilde{u})\right|\right|_2 u_T'(\tilde{t}) = 0 .$$

So we would not be able to control the speed of the vehicle, using the time-parameter function, in that point.

Note that, because of the way $u_T$ is defined, for each $u \in [a, b]$ the value $t_u$ exists and is unique. Further note that the velocity $v_T(t)$ depends on the time-parameter function, and is therefore not a geometric quantity, i.e., $v(u)$ is generally not equal to $\frac{ds}{du}(u)$.

## 2.3 Curvature

The curvature of a curve is a measure of how much the curve bends. This is a geometric quantity of the curve, and should therefore be a static quantity. We define the curvature with respect to the time $t$, and with respect to the curve parameter $u$, as the standard curvature for plane curves. Then we prove that these definitions are indeed consistent with each other, like we did for the distance. For convenience reasons we write $u_T$ for $u_T(t)$.

**Definition 2.5.** *Let $\mathbf{C}(u_T) = (x(u_T), y(u_T))$ be a twice continuously differentiable vehicle path. Then the curvature $\kappa_T(t)$ of the curve $\mathbf{C}(u_T)$ is*

$$\kappa_T(t) = \frac{\frac{dx}{dt}(u_T)\,\frac{d^2y}{dt^2}(u_T) - \frac{d^2x}{dt^2}(u_T)\,\frac{dy}{dt}(u_T)}{\left(\left(\frac{dx}{dt}(u_T)\right)^2 + \left(\frac{dy}{dt}(u_T)\right)^2\right)^{\frac{3}{2}}}\ , \quad t \in [t_a, t_b]\,.$$

*Let $\mathbf{C}(u) = (x(u), y(u))$ be a twice continuously differentiable vehicle path. Then the curvature $\kappa(u)$ of the curve $\mathbf{C}(u)$ is*

$$\kappa(u) = \frac{x'(u)\,y''(u) - x''(u)\,y'(u)}{\left(x'(u)\right)^2 + \left(y'(u)\right)^2\right)^{\frac{3}{2}}}\ , \quad u \in [a, b]\,.$$

**Theorem 2.2.** *The definitions of $\kappa_T(t)$ and $\kappa(u)$ are consistent with each other, i.e.,*

$$\kappa_T(t) = \kappa(u_T(t))\ .$$

*So the curvature is a static quantity.*

*Proof.* For the terms in the numerator we can write

$$\begin{aligned}
&\frac{dx}{dt}(u_T)\,\frac{d^2y}{dt^2}(u_T)\\
&= \left[\frac{dx}{du}(u_T)\,u_T'\right]\left[\frac{d}{dt}\left(\frac{dy}{du}(u_T)\,u_T'\right)\right]\\
&= \left[\frac{dx}{du}(u_T)\,u_T'\right]\left[\frac{d}{dt}\left(\frac{dy}{du}(u_T)\right)u_T' + \frac{dy}{du}(u_T)\,u_T''\right]\\
&= \left[\frac{dx}{du}(u_T)\,u_T'\right]\left[\frac{d^2y}{du^2}(u_T)\,{u_T'}^2 + \frac{dy}{du}(u_T)\,u_T''\right]\\
&= \left(\frac{dx}{du}(u_T)\,\frac{d^2y}{du^2}(u_T)\,{u_T'}^3\right) + \left(\frac{dx}{du}(u_T)\,\frac{dy}{du}(u_T)\,u_T'u_T''\right),
\end{aligned}$$

and following the same method

$$\begin{aligned}&\frac{d^2x}{dt^2}(u_T)\,\frac{dy}{dt}(u_T)\\ &\quad= \left(\frac{d^2x}{du^2}(u_T)\,\frac{dy}{du}(u_T)\,{u'_T}^3\right)+\left(\frac{dx}{du}(u_T)\,\frac{dy}{du}(u_T)\,u'_T u''_T\right).\end{aligned}$$

For the denominator we find

$$\begin{aligned}\left(\left(\frac{dx}{dt}(u_T)\right)^2+\left(\frac{dy}{dt}(u_T)\right)^2\right)^{\frac{3}{2}} &= \left(\left(\frac{dx}{du}(u_T)\right)^2{u'_T}^2+\left(\frac{dy}{du}(u_T)\right)^2{u'_T}^2\right)^{\frac{3}{2}}\\ &= \left(\left(\frac{dx}{du}(u_T)\right)^2+\left(\frac{dy}{du}(u_T)\right)^2\right)^{\frac{3}{2}}\left|u'_T\right|^3.\end{aligned}$$

Combining the above results, and using the nonnegativity of $u'_T(t)$, gives

$$\begin{aligned}\kappa_T(t) &= \frac{\left(\frac{dx}{du}(u_T)\,\frac{d^2y}{du^2}(u_T)\,{u'_T}^3\right)-\left(\frac{d^2x}{du^2}(u_T)\,\frac{dy}{du}(u_T)\,{u'_T}^3\right)}{\left(\left(\frac{dx}{du}(u_T)\right)^2+\left(\frac{dy}{du}(u_T)\right)^2\right)^{\frac{3}{2}}\left|u'_T\right|^3}\\ &= \operatorname{sgn}u'_T\,\frac{\left(\frac{dx}{du}(u_T)\,\frac{d^2y}{du^2}(u_T)\right)-\left(\frac{d^2x}{du^2}(u_T)\,\frac{dy}{du}(u_T)\right)}{\left(\left(\frac{dx}{du}(u_T)^2\right)+\left(\frac{dy}{du}(u_T)\right)^2\right)^{\frac{3}{2}}} \;=\; \kappa(u_T(t)).\end{aligned}$$

□

Note that for a vehicle path we have

$$\left|\left|\mathbf{C}'(u)\right|\right|_2=\left(\left(x'(u)\right)^2+\left(y'(u)\right)^2\right)^{\frac{1}{2}}\neq 0\ ,\quad u\in[a,b]\ .$$

Therefore $\kappa(u)$ is well defined, and, due to Theorem 2.2 above, so is $\kappa_T(t)$.

# 3 Vehicle Path Restrictions

Not all vehicle paths can be driven by any vehicle. For example, sharp turns could be a problem for some vehicles. In this section we introduce a simple vehicle model that we use as a guideline to the restrictions that are needed on a curve to ensure it can be used as a path. We explore what restrictions this model imposes, and how they influence vehicle paths. We will see that for the vehicle model used, the imposed vehicle restrictions translate to restrictions on the curvature and its derivative.

## 3.1 Vehicle Model

The model we use is that of a vehicle with three wheels, two rear wheels and one steering front wheel. Figure 1 below shows a schematic drawing of the vehicle model. There are three important parameters to this configuration

$\varphi$ : steering angle of the front wheel, $\varphi \in \left(-\frac{\pi}{2}, \frac{\pi}{2}\right)$,
$R$ : radius of curvature, $R > 0$,
$W$ : wheelbase, i.e., distance between front and rear axis, $W > 0$.

The radius of curvature $R$ is equal to one over the curvature, i.e., $R = 1/\kappa$.

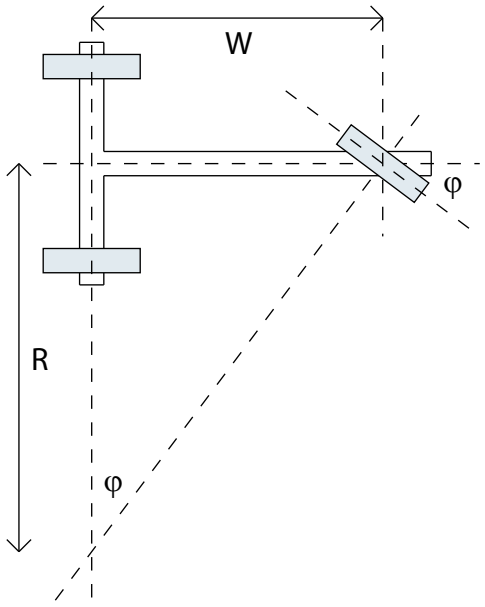


Figure 1: Vehicle Model for Curve Restrictions

### 3.2 Steering Angle Restriction

The most obvious restriction on the path of a vehicle, is a restriction on the steering angle at each point on the path

$$\varphi \in [\varphi_{\min}\,,\,\varphi_{\max}]\,. \tag{2}$$

We assume that $\varphi_{\min} \in [-2\pi, 0)$ and $\varphi_{\max} \in (0, 2\pi]$.

Since we have

$$\tan\varphi = \frac{W}{R} = W\kappa\,,$$

the restriction (2) on the steering angle $\varphi$ gives the following requirement for the curvature, which should be met on each point on the curve,

$$\kappa(u) \in \left[\frac{\tan\varphi_{\min}}{W}\,,\,\frac{\tan\varphi_{\max}}{W}\right]. \tag{3}$$

### 3.3 Steering Angular Velocity Restriction

We can extend the model, by imposing a restriction on the the angular velocity $\omega = d\varphi/dt$ of the steering mechanism

$$\omega \in [\omega_{\min}\,,\,\omega_{\max}]\,. \tag{4}$$

We assume that $\omega_{\min} < 0$ and $\omega_{\max} > 0$, because if these assumptions are not met the vehicle is not able to steer properly.

Unlike the steering angle restriction, which was static in each point, this is a dynamic restriction. Therefore we have to work with the time dependent curvature $\kappa_T(t)$.

For the angular velocity of the steering we can write

$$\omega(t) = \frac{d\varphi}{dt}(t) = \frac{d\arctan(W\kappa_T(t))}{dt} = \frac{W}{1+W^2(\kappa_T(t))^2}\frac{d\kappa_T(t)}{dt}\,.$$

Using that $\kappa_T(t) = \kappa(u_T(t))$ and Definition 2.4, we find

$$\begin{aligned}\omega(t) &= \frac{W}{1+W^2\kappa(u_T(t))^2}\,\frac{d\kappa}{du}(u_T(t))\,u_T'(t)\\ &= \frac{W}{1+W^2\kappa(u_T(t))^2}\,\frac{v_T(t)}{R(u_T(t))^{\frac{1}{2}}}\,\frac{d\kappa}{du}(u_T(t))\,,\end{aligned} \tag{5}$$

where

$$R(u) = \left|\left|\frac{d\mathbf{C}(u)}{du}\right|\right|_2^2\,.$$

Note that, since $W$, $v_T(t)$ and $R(u)$ are positive, for all $t$ we have

$$\operatorname{sgn}\omega(t) = \operatorname{sgn}\frac{d\kappa}{du}(u_T(t)) .$$

In the start point and endpoint we may have $u_T'(t) = 0$. Then by equation (5), $\omega(t) = 0$ in that point, and restriction (4) is automatically satisfied. For all $t$ for which $u_T'(t) \neq 0$ we can combine this restriction (4) with equation (5) to get

$$\frac{d\kappa}{du}(u_T(t)) \in \left[\omega_{\min}\frac{R^{\frac{1}{2}}}{v_T(t)}\,\frac{W^2\kappa^2+1}{W}\,,\,\omega_{\max}\frac{R^{\frac{1}{2}}}{v_T(t)}\,\frac{W^2\kappa^2+1}{W}\right], \qquad (6)$$

where $\kappa$ and $R$ denote $\kappa(u_T(t))$ and $R(u_T(t))$ respectively.

In practice, when we want to apply the angular velocity restriction to a vehicle path, $v_T(t)$ is usually not yet known. Therefore this constraint equation cannot be used as is. This does not render restriction (4) useless however.

A common practical constraint on a path, is that the vehicle should be able to drive along the path with a certain minimum speed

$$v_T(t) \geq v_{\min} > 0 . \qquad (7)$$

Combining this speed restriction with equation (6) we get

$$\frac{d\kappa}{du}(u_T(t)) \in \left[\omega_{\min}\frac{R^{\frac{1}{2}}}{v_{\min}}\,\frac{W^2\kappa^2+1}{W}\,,\,\omega_{\max}\frac{R^{\frac{1}{2}}}{v_{\min}}\,\frac{W^2\kappa^2+1}{W}\right],$$

where again $\kappa$ and $R$ denote $\kappa(u_T(t))$ and $R(u_T(t))$ respectively.

Substituting $u$ for $u_T(t)$, we effectively have a static constraint,

$$\kappa'(u) \in \left[\omega_{\min}\frac{R(u)^{\frac{1}{2}}}{v_{\min}}\,\frac{W^2\kappa(u)^2+1}{W}\,,\,\omega_{\max}\frac{R(u)^{\frac{1}{2}}}{v_{\min}}\,\frac{W^2\kappa(u)^2+1}{W}\right]. \qquad (8)$$

There is yet another way to use restriction (4). For all points in which $\frac{d\kappa}{du}(u_T(t)) \neq 0$, we can write equation (5) as

$$v_T(t) = \omega(t)\,R(u_T(t))^{\frac{1}{2}}\,\frac{W^2\kappa(u_T(t))^2+1}{W\frac{d\kappa}{du}(u_T(t))} .$$

Note that the right-hand side of this expression is always nonnegative.

Now, using $v_T(t) = v(u_T(t))$ and restriction (4), we find the following requirement for the velocity of the vehicle

$$v(u_T(t)) \in \begin{cases} \left[0\,,\,\omega_{\min}R^{\frac{1}{2}}\dfrac{W^2\kappa^2+1}{W\frac{d\kappa}{du}}\right] & , \quad \text{if } \frac{d\kappa}{du}(u_T(t)) < 0\,, \\ \left[0\,,\,\omega_{\max}R^{\frac{1}{2}}\dfrac{W^2\kappa^2+1}{W\frac{d\kappa}{du}}\right] & , \quad \text{if } \frac{d\kappa}{du}(u_T(t)) > 0\,, \end{cases}$$

where once again $\kappa$ and $R$ are functions of $u_T(t)$.

This is effectively a static constraint on the vehicle speed, at a point on a given vehicle path, due to a restriction on the angular velocity of the steering mechanism

$$v(u) \in \begin{cases} \left[0\,,\, \omega_{\min} R(u)^{\frac{1}{2}} \dfrac{W^2\kappa(u)^2+1}{W\frac{d\kappa}{du}(u)}\right] & , \quad \text{if } \frac{d\kappa}{du}(u) < 0\,, \\ \left[0\,,\, \omega_{\max} R(u)^{\frac{1}{2}} \dfrac{W^2\kappa(u)^2+1}{W\frac{d\kappa}{du}(u)}\right] & , \quad \text{if } \frac{d\kappa}{du}(u) > 0\,. \end{cases} \tag{9}$$

If $\frac{d\kappa}{du}(u) = 0$ then the angular velocity is also 0, i.e., the path is straight at that point, and there is no bound on the velocity $v(u)$ due to restriction on the angular velocity.

The velocity restriction (9) can be very useful in the application of heuristics that are based on the velocity of a vehicle along the path. For example, equation (9) gives us an upper bound for the velocity of the vehicle for all $u$. The maximum average speed the vehicle can achieve, driving the path, is given by the integral of the upper bound for the velocity, divided by the length of the path. This maximum average speed can be used as a measure of how good a path is for a vehicle.

# 4 B-Spline Paths

To apply the restrictions treated in Section 3 to a vehicle path, we need a mathematical representation of that path. As described in Section 1, our representation of choice is that of B-Spline curves.

**Definition 4.1.** *Let $m > 0$, and let a set $U = \{u_0, \ldots, u_m\}$ be given, with $u_i \in [a, b]$ nondecreasing and $u_0 = a$, $u_m = b$. We call $U$ the knot vector, and $u_i$ the knots. Let $0 \leq n < m$, and let a set of control points $P = \{\mathbf{P}_0, \ldots, \mathbf{P}_n\}$ be given, with $\mathbf{P}_i \in \mathbb{R}^d$. Define the degree $p$ as*

$$p := m - n - 1.$$

*A B-spline, given the control points $P$ and the knot vector $U$, is a curve*

$$\mathbf{C}(u) = \sum_{i=0}^{n} \mathbf{P}_i N_{i,p}(u) \quad , \quad u \in [a, b]$$

*where the basis functions $N_{i,p}(u)$, for $i \leq n$, are given by the recursive formula*

$$\begin{aligned} N_{i,0}(u) &= 1_{[u_i, u_{i+1})} = \begin{cases} 1 & , \quad u \in [u_i, u_{i+1}) \\ 0 & , \quad \textit{otherwise} \end{cases} \\ N_{i,k}(u) &= \frac{u - u_i}{u_{i+k} - u_i} N_{i,k-1}(u) + \frac{u_{i+k+1} - u}{u_{i+k+1} - u_{i+1}} N_{i+1,k-1}(u). \end{aligned}$$

*Note that $N_{i,k}$ can contain the quotient $\frac{0}{0}$. This quotient is defined to be $0$.*

For an overview of the relevant B-Spline theory see [Ide05]. For more information on B-Splines see [dB01] and [PT97].

From now on, with the term vehicle path we mean a vehicle path in B-Spline form that has basis functions that are three times continuously differentiable. This ensures that the derivative of the curvature as used in the steering angular velocity restriction (8), and later the repositioned version, exist.

To generate a good vehicle path we could randomly generate paths and hope to find a good one. Obviously, this is not a method we would like to use in practice. Instead, in Section 4.1 we introduce a convenient class of variations on a given vehicle path, parameterized by one variable $z$. This is the class of paths that has one control points repositioned with respect to the original path. We take special interest in the consequences for the curvature of vehicle paths, because the vehicle path restrictions treated in Section 3 depend on it. These consequences are treated in Section 4.2.

Our main focus is the repositioning of a single control point of a B-Spline. However, in Section 6 we introduce two extensions to this principle. We extend the repositioning to control points of NURBS curves, and treat the repositioning of multiple control points at once.

## 4.1 Repositioned Vehicle Path

Given a B-Spline vehicle path with three times continuously differentiable basis functions

$$\mathbf{C}(u) = \sum_{i=0}^{n} \mathbf{P}_i N_{i,p}(u) \ , \quad u \in [a,b] \ ,$$

we are going to reposition the $k^{\text{th}}$ control point $\mathbf{P}_k$ along a line through the original control point $\mathbf{P}_k$. From now on we presume the restriction $u \in [a,b]$, instead of explicitly noting it every time.

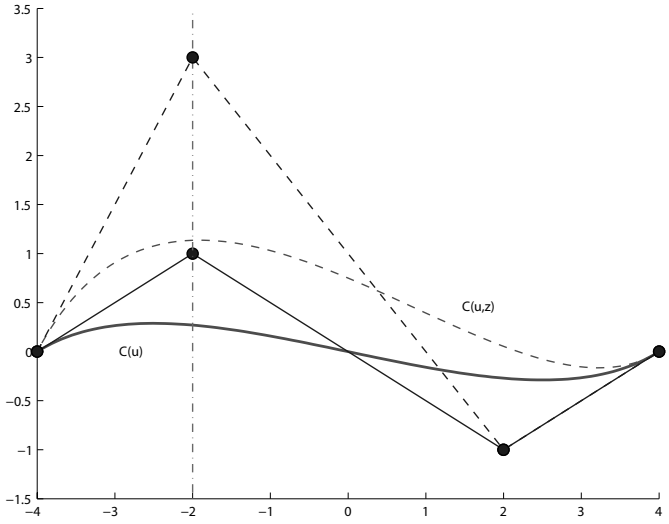


Figure 2: Control Point Repositioning

**Definition 4.2.** *Given a vehicle path* $\mathbf{C}(u)$*, a control point index* $k$*, and a reposition direction*

$$\boldsymbol{\alpha} = (\alpha_1, \alpha_2) \ , \ ||\boldsymbol{\alpha}||_2 = 1 \, ,$$

*we define the repositioned control points*

$$\begin{aligned} \bar{\mathbf{P}}_k &= \mathbf{P}_k + \boldsymbol{\alpha} z \quad , \ z \in \mathbb{R} \, , \\ \bar{\mathbf{P}}_i &= \mathbf{P}_i \qquad\quad , \ i \neq k \, . \end{aligned}$$

*Then the repositioned vehicle path is*

$$\mathbf{C}(u,z) = \sum_{i=0}^{n} \bar{\mathbf{P}}_i N_{i,p}(u) = \mathbf{C}(u) + \boldsymbol{\alpha} z N_{k,p}(u) \, .$$

*Further we define* $x(u,z)$ *and* $y(u,z)$ *to be the coordinates of the repositioned vehicle path,*

$$\mathbf{C}(u,z) = \begin{pmatrix} x(u,z) \\ y(u,z) \end{pmatrix} = \begin{pmatrix} x(u) + \alpha_1 z N_{k,p}(u) \\ y(u) + \alpha_2 z N_{k,p}(u) \end{pmatrix} .$$

Figure 2 above illustrates the control point repositioning principle. The solid curve and lines represent the original curve $\mathbf{C}(u)$ and its control polygon. The dashed curve and lines show the curve $\mathbf{C}(u,z)$ after a repositioning of the second from left control point along a vertical line.

## 4.2 Repositioned Vehicle Path Curvature

The curvature $\kappa(u,z)$ of the repositioned path $\mathbf{C}(u,z)$ is given by

$$\kappa(u,z) = \frac{\frac{\partial x(u,z)}{\partial u}\frac{\partial^2 y(u,z)}{\partial u^2} - \frac{\partial^2 x(u,z)}{\partial u^2}\frac{\partial y(u,z)}{\partial u}}{\left(\left(\frac{\partial x(u,z)}{\partial u}\right)^2 + \left(\frac{\partial y(u,z)}{\partial u}\right)^2\right)^{\frac{3}{2}}} .$$

Substituting the formula from Definition 4.2 and simplifying the expression, we get

$$\kappa(u,z) = \frac{S(u)\,z + T(u)}{\left(P(u)\,z^2 + Q(u)\,z + R(u)\right)^{\frac{3}{2}}} , \tag{10}$$

where

$$\begin{aligned}
P(u) &= \left(N'_{k,p}(u)\right)^2 , \\
Q(u) &= 2\left(\alpha_1 x'(u) + \alpha_2 y'(u)\right) N'_{k,p}(u) , \\
R(u) &= \left(x'(u)\right)^2 + \left(y'(u)\right)^2 = \left|\left|\mathbf{C}'(u)\right|\right|_2^2 , \\
S(u) &= \left(\alpha_1 y''(u) - \alpha_2 x''(u)\right) N'_{k,p}(u) - \left(\alpha_1 y'(u) - \alpha_2 x'(u)\right) N''_{k,p}(u) , \\
T(u) &= x'(u)\,y''(u) - x''(u)\,y'(u) .
\end{aligned}$$

Note that $P(u) \geq 0$ and $R(u) \geq 0$, and that $R(u)$ is the same as defined in Section 3.3. Further note that $\kappa(u) = T(u)/R(u)^{\frac{3}{2}}$.

By definition, for the basis functions we have

$$N_{k,p}(u) = 0 , \quad \text{for all } u \in [a, u_k) \cup [u_{k+p+1}, b] .$$

Since we have three times continuously differentiable basis functions

$$N_{k,p}(u) = N'_{k,p}(u) = N''_{k,p}(u) = 0 \text{ for all } u \in [a, u_k] \cup [u_{k+p+1}, b] . \tag{11}$$

Note the closure of the interval for $u$.

Using the equations (10) and (11), it follows that

$$\kappa(u,z) = \kappa(u) \text{ for all } u \notin (u_k, u_{k+p+1}) . \tag{12}$$

Therefore we can restrict our investigation of the influence of control point repositioning on the curvature to $u \in (u_k, u_{k+p+1})$. For such $u$ we define

$$\kappa_u(z) = \kappa(u,z) .$$

Based on the form of $\kappa_u(z)$ we distinguish a few different cases in our investigation of this function.

**Case** $N'_{k,p}(u) = 0$

B-Splines with $p = 0$ are not of interest, since they consist of only the control points. For $p > 0$ it is known from B-Spline theory that each basis function $N_{k,p}(u)$ attains exactly one maximum. Let this maximum be attained at $u = \bar{u}$. This parameter value $\bar{u}$ is the only point of interest in which $N'_{k,p}(u)$ is possibly equal to 0. Any other point for which $N'_{k,p}(u) = 0$ would necessarily be a minimum of $N_{k,p}(u)$, and the minimum value of a basis function is always 0. Due to the construction of the basis function, such a minimum can only be attained at $u = u_k$ or $u = u_{k+p+1}$, but we have already shown that $\kappa(u, z) = \kappa(u)$ at these points, see equation (12).

Note that it is not necessarily true that $N'_{k,p}(\bar{u}) = 0$. For example it is not true for all $k$ when $p = 1$, and for $p > 1$ in some cases when knots of multiplicity greater than 1 are involved.

Now assume that $u = \bar{u}$ and $N'_{k,p}(\bar{u}) = 0$, then the graph of $\kappa_u(z)$ is a line

$$\kappa_u(z) = \frac{S(u)\,z + T(u)}{R(u)^{\frac{3}{2}}} = \left(\frac{S(u)}{R(u)^{\frac{3}{2}}}\right) z + \kappa(u)\ . \tag{13}$$

See Figure 3 below for a graphical representation of this function. From equation (13) it is easy to see that $\kappa_u(0) = \kappa(u)$, and that $z_0 = -T/S$ is the unique value such that $\kappa_u(z_0) = 0$.

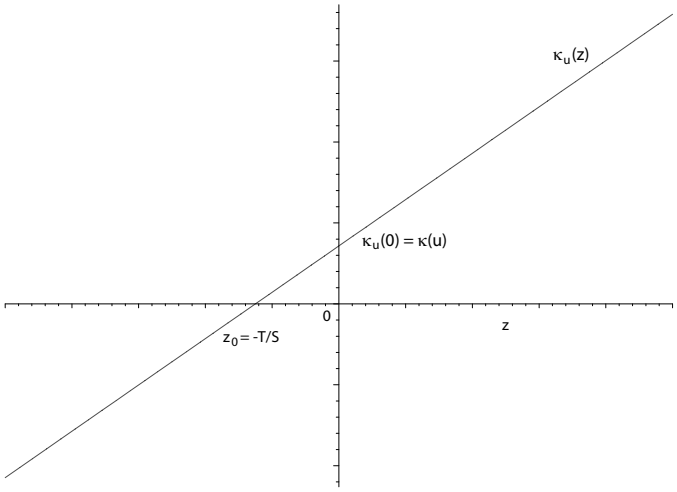


Figure 3: Curvature at $u$ when $N'_{k,p}(u) = 0$

**Case** $N'_{k,p}(u) \neq 0$

For all $u$ for which $N'_{k,p}(u) \neq 0$ the graph is slightly more complicated than it was for $N'_{k,p}(u) = 0$. The highest order of $z$ in the denominator is 3, which is higher than that of the numerator. Therefore the curvature $\kappa_u(z)$ goes to 0 for $z$ to $\pm\infty$.

If $N'_{k,p}(u) \neq 0$, the derivative of $\kappa_u(z)$ is given by

$$\begin{aligned} \frac{d\kappa_u(z)}{dz} &= \frac{2S\left(Pz^2+Qz+R\right)-3\left(Sz+T\right)\left(2Pz+Q\right)}{2\left(Pz^2+Qz+R\right)^{\frac{5}{2}}} \\ &= -\frac{\left(4PS\right)z^2+\left(6PT+QS\right)z+\left(3QT-2RS\right)}{2\left(Pz^2+Qz+R\right)^{\frac{5}{2}}}\,. \end{aligned} \tag{14}$$

For convenience we have left out the dependence of $P$, $Q$, $R$, $S$ and $T$ on $u$ in the above expression.

Suppose that $S(u) = 0$. If $T(u) = 0$ then simply $\kappa_u(z) = 0$ for all $z$, so let us suppose that $T(u) \neq 0$. Then we have

$$\kappa_u(z) = \frac{T}{\left(Pz^2+Qz+R\right)^{\frac{3}{2}}}\,, \tag{15}$$

and

$$\frac{d\kappa_u(z)}{dz} = -\frac{6PTz+3QT}{2\left(Pz^2+Qz+R\right)^{\frac{5}{2}}}\,. \tag{16}$$

From equation (15) it easily follows that, if $S(u) = 0$, the function $\kappa_u(z)$ has no root. And by equation (16) its derivative has exactly one root

$$\frac{d\kappa_u(z)}{dz} = 0 \Leftrightarrow z = -\frac{Q}{2P}\,. \tag{17}$$

Therefore $\kappa_u(z)$ does not intersect the $x$-axis, and has exactly one extreme value, which is a global maximum for $T(u) > 0$ and a global minimum for $T(u) < 0$. This extreme value is

$$\kappa_{ext} = \kappa_u\left(\frac{-Q}{2P}\right) = \frac{T}{\left(R-\frac{Q^2}{4P}\right)^{\frac{3}{2}}}\,. \tag{18}$$

Further we can prove that $\kappa_u(z)$ is symmetrical around $z = \frac{-Q}{2P}$, as follows

$$\begin{aligned}
\kappa_u\left(\xi - \frac{Q}{2P}\right) &= \frac{T}{\left[P\left(\xi^2 - \frac{Q}{P}\xi + \frac{Q^2}{4P}\right) + Q\left(\xi - \frac{Q}{2P}\right) + R\right]^{\frac{3}{2}}} \\
&= \frac{T}{\left[P\xi^2 - Q\xi + \frac{Q^2}{4} + Q\xi - \frac{Q^2}{2P} + R\right]^{\frac{3}{2}}} \\
&= \frac{T}{\left[P\xi^2 + \frac{Q^2}{4} - \frac{Q^2}{2P} + R\right]^{\frac{3}{2}}} .
\end{aligned}$$

The value of this expression is the same for $\xi$ and $-\xi$, hence $\kappa_u(z)$ is symmetrical around $z = \frac{-Q}{2P}$.

From these facts we can conclude that the graph of $\kappa_u(z)$ typically has the shape shown in Figure 4 below. Note that the presented graph is for the case $T(u) > 0$.

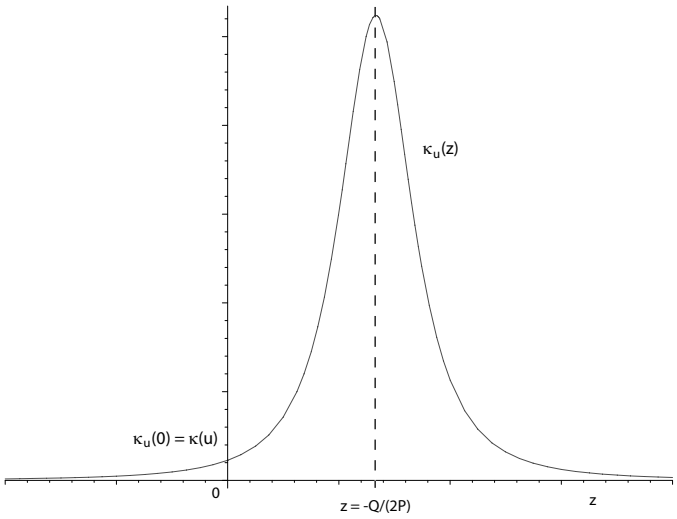


Figure 4: Curvature at $u$ when $N'_{k,p}(u) \neq 0$, $S(u) = 0$ and $T(u) > 0$

When $S(u) \neq 0$, then $\kappa_u(z)$ has exactly one root

$$\kappa_u(z) = 0 \Leftrightarrow z = -\frac{T}{S} .$$

The roots of the derivative can be found using

$$\begin{aligned}
\frac{d\kappa_u(z)}{dz} = 0 \quad &\Leftrightarrow \quad (4PS)z^2 + (6PT + QS)z + (3QT - 2RS) = 0 \\
&\Leftrightarrow \quad z_{1,2} = \frac{-(6PT+QS) \pm \sqrt{(6PT+QS)^2 - (16PS)(3QT-2RS)}}{8PS} . \quad (19)
\end{aligned}$$

From the facts that $\kappa_u(z)$ goes to 0 for $z$ to $\pm\infty$, and that it intersects the $x$-axis at exactly one point, combined with the absence of vertical asymptotes because $Pz^2 + Qz + R > 0$, it follows that the graph must attain exactly one maximum and one minimum. The values of $z$ at which these extreme values are found, are necessarily the solutions of equation (19). Therefore these solutions must be real valued.

We can also proof this mathematically.

**Lemma 4.1.** *Given that $P, Q, R, S, T \in \mathbb{R}$, $P > 0$ and $Pz^2 + Qz + R \geq 0$ for all $z$, the values*

$$z_{1,2} = \frac{-(6PT + QS) \pm \sqrt{\Delta}}{8PS},$$

*with $\Delta$ the polynomial discriminant*

$$\Delta = (6PT + QS)^2 - (16PS)(3QT - 2RS),$$

*are real numbers.*

*Proof.* Since $P, Q, R, S, T \in \mathbb{R}$ it only remains to be shown that $\Delta \geq 0$, i.e.,

$$\begin{aligned} z_{1,2} \in \mathbb{R} &\Leftrightarrow (6PT + QS)^2 - (16PS)(3QT - 2RS) \geq 0 \\ &\Leftrightarrow 36P^2T^2 - 36PQST + Q^2S^2 + 32PRS^2 \geq 0 \end{aligned}$$

Using that $Pz^2 + Qz + R \geq 0$ for all $z$, we continue by eliminating $R$ from of this equation, and rewriting the remaining equation to a square, which is of course non-negative.

From $Pz^2+Qz+R \geq 0$ for all $z$ it follows that the equation $Pz^2+Qz+R = 0$ has at most one solution. This is true if and only if the discriminant of that quadratic equation is non-positive, i.e.,

$$Q^2 - 4PR \leq 0 \;\Leftrightarrow\; 4PR \geq Q^2.$$

Therefore we can write

$$\begin{aligned} \Delta &= 36P^2T^2 - 36PQST + Q^2S^2 + 32PRS^2 &\geq \\ &\quad 36P^2T^2 - 36PQST + Q^2S^2 + 8Q^2S^2 &= \\ &\quad 9\left(4P^2T^2 - 4PQST + Q^2S^2\right) &= \\ &\quad 9(2PT - QS)^2 &\geq 0. \end{aligned}$$

□

We now have enough information to derive the typical shape of the graph of $\kappa_u(z)$ for $S(u) \neq 0$. Figure 5 below shows this shape for $S(u) < 0$.

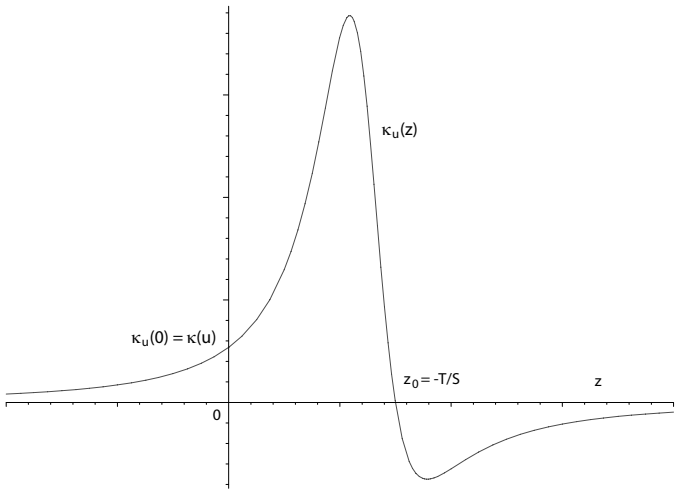


Figure 5: Curvature at $u$ when $N'_{k,p}(u) \neq 0$ and $S(u) \neq 0$

# 5 B-Spline Path Restrictions

In Section 3 we derived the steering angle restriction (3), and the steering angular velocity restriction (6). A vehicle path has to satisfy both these equations, in order for a vehicle to be able to drive the path.

In this section we apply these restrictions to the class $\mathbf{C}(u, z)$ of repositioned vehicle paths, for some given $\mathbf{C}(u)$, $k$, and $\boldsymbol{\alpha}$. We use our knowledge of the curvature of the repositioned vehicle path, to calculate what choices $z = \tilde{z}$ give a path $\mathbf{C}(u, \tilde{z})$ that satisfies the path restrictions. But we start with a definition of a curvature restriction, and the feasible repositioning set.

**Definition 5.1.** *A curvature restriction $\mathcal{R}(q, \mu, \nu)$ is a condition*

$$\mu(u, z) \leq \frac{\partial^q \kappa}{\partial u^q}(u, z) \leq \nu(u, z) \ .$$

*It is allowed that either $\mu(u, z) = -\infty$ or $\nu(u, z) = \infty$, but not both.*

*We say that $\tilde{z}$ satisfies the curvature restriction $\mathcal{R}(q, \mu, \nu)$ for $\tilde{u}$, if the condition is met for $u = \tilde{u}$ when $z = \tilde{z}$.*

*The feasible repositioning set $\mathcal{F}(q, \mu, \nu)$, is the set of all $z$ that satisfy the curvature restriction $\mathcal{R}(q, \mu, \nu)$ for all $u$.*

The problem of finding the feasible repositioning set $\mathcal{F}(q, \mu, \nu)$ is generally too complex to solve analytically. Therefore we discretize the problem in the $u$ direction. That is, for each $v_i$ in a finite discretization set $V = \{v_i\}$, with $v_i \in [a, b]$ for all $i$, we calculate the set $F_{v_i}$ of all $z$ that satisfy the restriction $\mathcal{R}(q, \mu, \nu)$ for $u = v_i$.

The reason that we discretize in the $u$ direction, instead of the $z$ direction, is that the curvature of a repositioned vehicle path is a very complex expression of $u$, but it is a fairly simple expression of $z$.

Now let us define the intersection $F_V$ of all $F_{v_i}$,

$$F_V = \textstyle\bigcap_i F_{v_i} \ .$$

We then have

$$\mathcal{F}(q, \mu, \nu) \subseteq F_V \ .$$

In our application $\kappa(u, z)$ should be a smooth function, and we also intend to use smooth functions $\mu(u, z)$ and $\nu(u, z)$. Therefore, in practice, $F_V$ will be a good approximation of $\mathcal{F}(q, \mu, \nu)$, provided that we choose an appropriate set discretization $V$.

## 5.1 Steering Angle Restriction

The simplest curvature restriction is a lower and upper bound on the curvature, i.e.,

$$\mathcal{R}_0 = \mathcal{R}\left(0, \mu_0, \nu_0\right) \text{ with } \mu_0, \nu_0 \in \mathbb{R}\,. \tag{20}$$

Taking $\mu_0 = \tan\varphi_{\min}/W$ and $\nu_0 = \tan\varphi_{\max}/W$, this is exactly restriction (3) applied to a set of repositioned curves, which yields bounds on the steering angle of the vehicle. Because of this application we assume that $\mu_0 < 0$ and $\nu_0 > 0$.

Since lower and upper bounds can be treated in the same way, we only concern ourselves with the upper bound problem. To find the set $F_u$ of all $z$ that satisfy $\mathcal{R}_0$ for $u$, we therefore have to solve the following equation

$$\kappa_u\left(z\right) \leq \nu_0 \ , \ \nu_0 > 0\,.$$

We distinguish the cases $N'_{k,p}\left(u\right) = 0$, and $N'_{k,p}\left(u\right) \neq 0$ with either $S\left(u\right) = 0$ or $S\left(u\right) \neq 0$. For simplicity reasons we drop the dependence of $P$, $Q$, $R$, $S$ and $T$ from $u$ in notations for the remainder of this section.

**Case** $N'_{k,p}\left(u\right) = 0$

Using equation (13), the equation we have to solve to find $F_u$ is

$$\kappa_u\left(z\right) = \frac{Sz+T}{R^{\frac{3}{2}}} \leq \nu_0 \ \Leftrightarrow \ Sz \leq \nu_0 R^{\frac{3}{2}} - T\,.$$

We then have to distinguish the following possibilities

$$\begin{aligned}
S = 0 \ &\Rightarrow \ \begin{cases} F_u \ = \ \mathbb{R} \ , \ \text{if} \ \ \nu_0 R^{\frac{3}{2}} \geq T \\ F_u \ = \ \emptyset \ , \ \text{otherwise} \end{cases} \\
S < 0 \ &\Rightarrow \ F_u \ = \ \left[\frac{\nu_0 R^{\frac{3}{2}} - T}{S}, \infty\right) \\
S > 0 \ &\Rightarrow \ F_u \ = \ \left(-\infty, \frac{\nu_0 R^{\frac{3}{2}} - T}{S}\right]\,.
\end{aligned}$$

As described in Section 4.2, there is at most one value $\bar{u} \in (u_k, u_{k+p+1})$ for which $N'_{k,p}\left(\bar{u}\right) = 0$. Therefore it will almost never be in our discretization set $V$. This $\bar{u}$ is still of significant value though. As we will see, for all other $u$ very large positive and very large negative values of $z$ are always feasible. By adding $\bar{u}$ to our discretization set $V$ we can make sure that the large values of $z$ are removed from the feasible interval, as they should be.

**Case $N'_{k,p}(u) \neq 0$ and $S(u) = 0$**

In this case the the equation we have to solve to find $F_u$ becomes

$$\kappa_u(z) = \frac{T}{(Pz^2 + Qz + R)^{\frac{3}{2}}} \leq \nu_0 .$$

Using the typical shape of $\kappa_u(z)$ in this case, as shown in Figure 4, we can immediately see that

$$T \leq 0 \quad \Rightarrow \quad F_u = \mathbb{R} .$$

If $T > 0$ then $\kappa_u(z)$ has exactly one maximum value. By equation (17) this maximum of the curvature $\kappa_u(z)$ is

$$\kappa_u^{max} = \kappa_u\left(\frac{-Q}{2P}\right) = \frac{T}{\left(-\frac{Q^2}{4P} + R\right)^{\frac{3}{2}}} .$$

It is easy to see that

$$\begin{aligned} T > 0 \text{ and } \nu_0 \geq \kappa_u^{max} \quad &: \quad F_u \;=\; \mathbb{R} \\ T > 0 \text{ and } \nu_0 < \kappa_u^{max} \quad &: \quad F_u \;=\; (-\infty, z_1] \cup [z_2, \infty) \;, \end{aligned}$$

where $z_1$ and $z_2$ are the solutions of the equation $\kappa_u(z) = \nu_0$, with $z_1 < z_2$.

Note that in the described situation $T > 0$ and $\nu_0 \in (0, \kappa_u^{max})$, the equation $\kappa_u(z) = \nu_0$ has indeed exactly two unique solutions $z_1$ and $z_2$. Further note that, since $\kappa_u(z)$ is symmetric with respect to $z = -Q/(2P)$, we can write $z_1 = -Q/(2P) - \xi$ and $z_1 = -Q/(2P) + \xi$ for some $\xi > 0$.

**Case $N'_{k,p}(u) \neq 0$ and $S(u) \neq 0$**

The equation we have to solve in order to find $F_u$ becomes

$$\kappa_u(z) = \frac{Sz + T}{(Pz^2 + Qz + R)^{\frac{3}{2}}} \leq \nu_0 .$$

The curvature $\kappa_u(z)$ has two extreme values, one of which is a maximum. Using equation (19) we see that this maximum is attained at

$$\begin{aligned} \bar{z} &= \frac{-(6PT + QS) - \sqrt{\Delta}}{8PS} \quad \text{for} \quad S < 0 , \\ \bar{z} &= \frac{-(6PT + QS) + \sqrt{\Delta}}{8PS} \quad \text{for} \quad S > 0 , \end{aligned}$$

where

$$\Delta = (6PT + QS)^2 - (16PS)(3QT - 2RS) .$$

Let $\kappa_u^{max}$ denote the maximum value of $\kappa_u(z)$, i.e.,

$$\kappa_u^{max} = \kappa_u(\bar{z}) \ .$$

Again, it easily follows that

$$\begin{array}{lcl} T > 0 \text{ and } \nu_0 \geq \kappa_u^{max} & : & F_u = \mathbb{R} \\ T > 0 \text{ and } \nu_0 < \kappa_u^{max} & : & F_u = (-\infty, z_1] \cup [z_2, \infty) \ , \end{array}$$

where $z_1$ and $z_2$ are the solutions of the equation $\kappa_u(z) = \nu_0$, with $z_1 < z_2$.

Note that in the described situation $T > 0$ and $\nu_0 \in (0, \kappa_u^{max})$, the equation $\kappa_u(z) = \nu_0$ indeed has exactly two unique solutions $z_1$ and $z_2$.

## 5.2 Steering Angular Velocity Restriction

The angular velocity restriction (6) on the steering mechanism, applied to a repositioned curve $\mathbf{C}(u, z)$, yields the following curvature restriction

$$\mathcal{R}_1 = \mathcal{R}(1, \mu_1, \nu_1) \text{ with } \mu, \nu \in \mathbb{R} \,, \tag{21}$$

where

$$\begin{aligned} \mu_1(u,z) &= \omega_{\min} \frac{R(u,z)^{\frac{1}{2}}}{v_{\min}} \frac{W^2 \kappa(u,z)^2 + 1}{W} \,, \\ \nu_1(u,z) &= \omega_{\max} \frac{R(u,z)^{\frac{1}{2}}}{v_{\min}} \frac{W^2 \kappa(u,z)^2 + 1}{W} \,, \end{aligned}$$

with

$$R(u,z) = \left|\left| \frac{\partial \mathbf{C}}{\partial u}(u,z) \right|\right|_2^2 = P(u) z^2 + Q(u) z + R(u) \ .$$

Again since lower and upper bounds can be treated in the same way, we only discuss the upper bound problem, i.e.,

$$\frac{\partial \kappa}{\partial u}(u,z) \leq \nu_1(u,z) \,.$$

Writing out the expression for $\frac{\partial \kappa}{\partial u}(u,z)$ gives

$$\frac{\partial \kappa}{\partial u}(u,z) = \frac{(S'z + T')\left(Pz^2 + Qz + R\right) - \frac{3}{2}(Sz+T)\left(P'z^2 + Q'z + R'\right)}{(Pz^2 + Qz + R)^{\frac{5}{2}}} \ ,$$

and when we write out $\nu_1(u,z)$ we get

$$\begin{aligned}
\nu_1(u,z) &= \frac{\omega_{\max}}{v_{\min}} R(u,z)^{\frac{1}{2}} \left( W\kappa(u,z)^2 + \frac{1}{W} \right) \\
&= \frac{\omega_{\max}}{v_{\min}} \left( Pz^2 + Qz + R \right)^{\frac{1}{2}} \left[ \frac{W(Sz+T)^2}{(Pz^2+Qz+R)^3} + \frac{1}{W} \right] \\
&= \frac{\omega_{\max}}{v_{\min}} \left[ \frac{W(Sz+T)^2 + \frac{1}{W}\left(Pz^2+Qz+R\right)^3}{(Pz^2+Qz+R)^{\frac{5}{2}}} \right].
\end{aligned}$$

Out of convenience we are leaving out the dependence of $P$, $Q$, $R$, $S$, and $T$ on $u$ in the notation.

Combining the above three equations, it follows that

$$\begin{aligned}
&\frac{\partial \kappa}{\partial u}(u,z) \leq \nu_1(u,z) \Leftrightarrow \\
&\left(S'z+T'\right)\left(Pz^2+Qz+R\right) - \frac{3}{2}(Sz+T)\left(P'z^2+Q'z+R'\right) \leq \\
&\qquad \frac{\omega_{\max}}{v_{\min}} \left[ W(Sz+T)^2 + \frac{1}{W}\left(Pz^2+Qz+R\right)^3 \right].
\end{aligned}$$

Some simple, though tedious, calculations show that the equality of the above expression is equivalent to

$$\sum_{i=0}^{6} \rho_i z^i = 0\,, \tag{22}$$

where

$$\begin{aligned}
\rho_0 &= \tfrac{\omega_{\max}}{v_{\min}} \left( \tfrac{1}{W} R^3 + WT^2 \right) + \tfrac{3}{2} R'T - RT'\,, \\
\rho_1 &= \tfrac{\omega_{\max}}{v_{\min}} \left( \tfrac{3}{W} QR^2 + 2WST \right) + \tfrac{3}{2} Q'T - QT' + \tfrac{3}{2} R'S - RS'\,, \\
\rho_2 &= \tfrac{\omega_{\max}}{v_{\min}} \left( \tfrac{3}{W} \left( PR^2 + Q^2 R \right) + WS^2 \right) + \tfrac{3}{2} P'T - PT' + \tfrac{3}{2} Q'S - QS'\,, \\
\rho_3 &= \tfrac{\omega_{\max}}{v_{\min}} \left( \tfrac{1}{W} \left( 6PQR + Q^3 \right) \right) + \tfrac{3}{2} P'S - PS'\,, \\
\rho_4 &= \tfrac{\omega_{\max}}{v_{\min}} \left( \tfrac{3}{W} \left( P^2 R + PQ^2 \right) \right), \\
\rho_5 &= \tfrac{\omega_{\max}}{v_{\min}} \left( \tfrac{3}{W} P^2 Q \right), \\
\rho_6 &= \tfrac{\omega_{\max}}{v_{\min}} \left( \tfrac{1}{W} P^3 \right).
\end{aligned}$$

In other words, we have to find the roots of a polynomial of degree 6 in $z$. These roots can be calculated with a numerical root finding algorithm. From these roots it is easy to determine the intervals for $z$, on which the original inequality $\frac{\partial \kappa}{\partial u}(u,z) \leq \nu_1(u,z)$ holds for the chosen value of $u$.

# 6 Extended Repositioning

As mentioned in Section 4, our main focus is the repositioning of a single control point of a B-Spline. However, the work done in Section 4 and 5 is quite easily extended to the repositioning of control points of NURBS curves, and to the repositioning of multiple control points at once.

In this section we introduce both extensions, following the same ideas as for the repositioning of a single control point of a B-Spline. And we show that the work on vehicle path restrictions from Section 5 is almost directly applicable on these extensions.

## 6.1 NURBS Vehicle Path Repositioning

A NURBS curve is a Non-Uniform Rational B-Spline curve, i.e., a B-spline on a nonuniform knot vector with rational basis functions.

**Definition 6.1.** *Let $m > 0$, and let a knot vector $U = \{u_0, \ldots, u_m\}$ be given, with $u_i \in [a, b]$ nondecreasing and $u_0 = a$, $u_m = b$. Let $0 \leq n < m$, and let a set of weights $W = \{w_0, \ldots, w_n\}$, with $w_i > 0$, and a set of control points $P = \{\mathbf{P}_0, \ldots, \mathbf{P}_n\}$ be given, with $\mathbf{P}_i \in \mathbb{R}^d$. Define the degree $p$ as*

$$p := m - n - 1.$$

*A NURBS curve, given control points $P$, knot vector $U$ and weights $W$, is a curve*

$$\mathbf{C}(u) = \sum_{i=0}^{n} \mathbf{P}_i R_{i,p}(u) \quad , \quad u \in [a, b] \ ,$$

*where the rational basis functions $R_{i,p}$ are given by*

$$R_{i,p}(u) = \frac{N_{i,p}(u)\, w_i}{\sum_{j=0}^{n} N_{j,p}(u)\, w_j} \ .$$

*with $N_{i,p}$ the standard B-spline basis functions.*

NURBS are more flexible than ordinary B-Splines. Every possible B-Spline can also be described as a NURBS curve, by using the same control points and setting all weights equal to 1. And a lot of curves that cannot be described as B-Splines, can be captured as NURBS curves. Therefore it could be beneficial to work with vehicle paths in NURBS form, rather than in B-Spline form. For an overview of the relevant NURBS theory see [Ide05]. For more information on NURBS curves see [PT97].

The extension of the definition of control point repositioning to a NURBS vehicle path is straightforward.

**Definition 6.2.** *Given a NURBS vehicle path* $\mathbf{C}(u)$ *with three times continuously differentiable basis functions, a control point index* $k$*, and a reposition direction*

$$\boldsymbol{\alpha} = (\alpha_1, \alpha_2) \ , \ ||\boldsymbol{\alpha}||_2 = 1 \, ,$$

*we define the repositioned control points*

$$\begin{aligned} \bar{\mathbf{P}}_k &= \mathbf{P}_k + \boldsymbol{\alpha} z \quad , \ z \in \mathbb{R} \, , \\ \bar{\mathbf{P}}_i &= \mathbf{P}_i \qquad\quad , \ i \neq k \, . \end{aligned}$$

*Then the repositioned vehicle path is*

$$\mathbf{C}(u, z) = \sum_{i=0}^{n} \bar{\mathbf{P}}_i R_{i,p}(u) = \mathbf{C}(u) + \boldsymbol{\alpha} z R_{k,p}(u) \, .$$

*Further we define* $x(u, z)$ *and* $y(u, z)$ *to be the coordinates of the repositioned vehicle path,*

$$\mathbf{C}(u, z) = \begin{pmatrix} x(u, z) \\ y(u, z) \end{pmatrix} = \begin{pmatrix} x(u) + \alpha_1 z R_{k,p}(u) \\ y(u) + \alpha_2 z R_{k,p}(u) \end{pmatrix} .$$

Substituting the formula from Definition 6.2 into the curvature, like we did for B-Splines in Section 4.2, we again get

$$\kappa(u, z) = \frac{S(u) z + T(u)}{\left(P(u) z^2 + Q(u) z + R(u)\right)^{\frac{3}{2}}} \ ,$$

but now with

$$\begin{aligned} P(u) &= \left(R'_{k,p}(u)\right)^2 \, , \\ Q(u) &= 2\left(\alpha_1 x'(u) + \alpha_2 y'(u)\right) R'_{k,p}(u) \, , \\ R(u) &= \left(x'(u)\right)^2 + \left(y'(u)\right)^2 = \left|\left|\mathbf{C}'(u)\right|\right|_2^2 \, , \\ S(u) &= \left(\alpha_1 y''(u) - \alpha_2 x''(u)\right) R'_{k,p}(u) - \left(\alpha_1 y'(u) - \alpha_2 x'(u)\right) R''_{k,p}(u) \, , \\ T(u) &= x'(u) y''(u) - x''(u) y'(u) \, . \end{aligned}$$

As in Section 4.2 we have $P(u) \geq 0$ and $R(u) \geq 0$.

By definition, for the NURBS basis functions we have

$$R_{k,p}(u) = 0 \, , \quad \text{for all } u \in [a, u_k) \cup [u_{k+p+1}, b] \, .$$

Following the same reasoning as for the B-Spline case we find that we can restrict our investigation of the influence of control point repositioning on the curvature, to $u \in (u_k, u_{k+p+1})$.

All calculations for the vehicle restrictions, that we have done in Section 4 and 5, are in terms of $P(u)$, $Q(u)$, $R(u)$, $S(u)$ and $T(u)$. With the above described properties of these functions the results for the calculation of feasible repositioning sets remain valid, independent of the exact form of these functions. The only exception is the distinction we make between the cases $N'_{k,p}(u) = 0$ and $N'_{k,p}(u) \neq 0$. For NURBS vehicle paths, this translates into distinguishing the cases $R'_{k,p}(u) = 0$ and $R'_{k,p}(u) \neq 0$.

## 6.2 Multiple Control Point Repositioning

Instead of repositioning a single control point of a NURBS curve in a certain direction, given by the reposition direction $\boldsymbol{\alpha}$, we can also reposition multiple control points into that direction.

**Definition 6.3.** *Given a NURBS vehicle path $\mathbf{C}(u)$ with three times continuously differentiable basis functions, a control point index $k$, and a reposition direction*

$$\boldsymbol{\alpha} = (\alpha_1, \alpha_2) \ , \ ||\boldsymbol{\alpha}||_2 = 1 \, ,$$

*we define the repositioned control points*

$$\bar{\mathbf{P}}_i = \mathbf{P}_i + \zeta_i \boldsymbol{\alpha} z \quad , \ z \in \mathbb{R} \, , \ \zeta_i \in [-1, 1] \ , \ i = 0, \ldots, n \, .$$

*Then the repositioned vehicle path is*

$$\mathbf{C}(u, z) = \sum_{i=0}^{n} \bar{\mathbf{P}}_i R_{i,p}(u) = \mathbf{C}(u) + \boldsymbol{\alpha} z \sum_{i=0}^{n} \zeta_i R_{i,p}(u) \, .$$

*Further we define $x(u, z)$ and $y(u, z)$ to be the coordinates of the repositioned vehicle path,*

$$\mathbf{C}(u, z) = \begin{pmatrix} x(u, z) \\ y(u, z) \end{pmatrix} = \begin{pmatrix} x(u) + \alpha_1 z \sum_{i=0}^{n} \zeta_i R_{i,p}(u) \\ y(u) + \alpha_2 z \sum_{i=0}^{n} \zeta_i R_{i,p}(u) \end{pmatrix} .$$

Again we can write

$$\kappa(u, z) = \frac{S(u) z + T(u)}{\left(P(u) z^2 + Q(u) z + R(u)\right)^{\frac{3}{2}}} \ ,$$

but for multiple control point repositioning we have

$$\begin{aligned}
P(u) &= \left(\textstyle\sum_{i=0}^{n} \zeta_i R'_{i,p}(u)\right)^2 \, , \\
Q(u) &= 2\left(\alpha_1 x'(u) + \alpha_2 y'(u)\right) \textstyle\sum_{i=0}^{n} \zeta_i R'_{i,p}(u) \ , \\
R(u) &= \left(x'(u)\right)^2 + \left(y'(u)\right)^2 = \left|\left|\mathbf{C}'(u)\right|\right|_2^2 \, , \\
S(u) &= \left(\alpha_1 y''(u) - \alpha_2 x''(u)\right) \textstyle\sum_{i=0}^{n} \zeta_i R'_{i,p}(u) \\
&\quad - \left(\alpha_1 y'(u) - \alpha_2 x'(u)\right) \textstyle\sum_{i=0}^{n} \zeta_i R''_{i,p}(u) \ , \\
T(u) &= x'(u) y''(u) - x''(u) y'(u) \ .
\end{aligned}$$

As before we have $P(u) \geq 0$ and $R(u) \geq 0$, and it is simple to see that we can restrict our investigation to

$$u \in \bigcup_{i \in I^+} (u_i, u_{i+p+1}) \ ,$$

where

$$I^+ = \{i \in \{0, \ldots, n\} \mid \zeta_i > 0\} \ .$$

So we can also directly use the results from Section 4 and 5 for curves with multiple repositioned control points, as long as the control points are repositioned in the same direction $\boldsymbol{\alpha}$. The distinction we originally made between the cases $N'_{k,p}(u) = 0$ and $N'_{k,p}(u) \neq 0$, translates into distinguishing the cases $\sum_{i=0}^{n} \zeta_i R'_{i,p}(u) = 0$ and $\sum_{i=0}^{n} \zeta_i R'_{i,p}(u) \neq 0$ when dealing with multiple repositioned control points.

Note that, if multiple control points would be repositioned in different directions, an extra term $M(u) z^2$, that is generally nonzero, would appear in the numerator of the curvature function $\kappa(u, z)$. In that case the results of Section 4 and 5 would no longer be applicable to the repositioned curve.

Further note that it is obvious that we can also use these results to work with B-Splines with multiple repositioned control points, since NURBS curves are an extension of B-Splines.

# 7 Path Construction

In this section we research a practical application of the theory and methods we developed in the previous sections. The goal is to develop a method that can be used to construct feasible paths for a vehicle and is easy to use.

The general idea of the path construction method is this. We start with a linear approximation of the path we want the vehicle to drive. Next we choose pairs of points between which we want the linear path to be rounded to create bends. Figure 6 shows an example of a linear path approximation in black, with rounded bends between chosen endpoints in red.

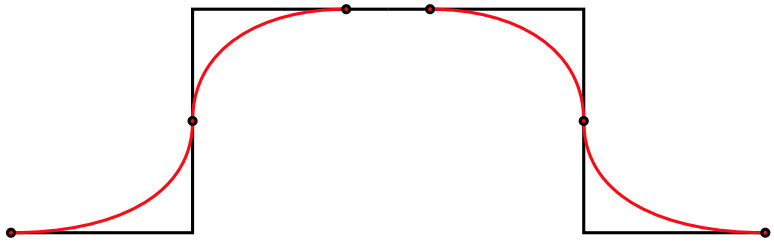

Figure 6: Single Corner Application

Thus, given two endpoints $\mathbf{E}_1$ and $\mathbf{E}_2$ on two different line segments, we want to construct a B-Spline curve between the endpoints that is straight at these endpoints, and has the same direction as the line segment the endpoint is on. This is because the bend curve has to fit geometrically to the part of a line segment that is not rounded, allowing us to combine the curve and such straight parts, or other bend curves, to one single path.

First we introduce a control point scheme for the construction of a single bend curve between two given endpoints, and we explore the parameters of this construction scheme. Then we show how to connect multiple single bends to a larger path curve, and we discuss how to safeguard the feasibility of the path we are constructing. Finally we discuss some extensions and alternatives to the presented construction method.

## 7.1 Single Bend Curve Construction

When constructing a bend curve for a vehicle path, obviously the curve needs to satisfy the general requirements for a vehicle path, i.e, it has to be three times continuously differentiable in all points, including the endpoints. Therefore we use a B-Spline curve with degree $p = 4$, and a uniform knot vector. Note that to get a three times continuously differentiable vehicle path it would be enough to have no internal knot with multiplicity larger than

1, but we will need the uniformness of the knot vector later. Furthermore we assume that the curve parameter $u \in [0, 1]$, but the results are easily extended to B-Splines with a curve parameter $u \in [a, b]$.

For the curve to be a valid vehicle path we assume that the norm of the derivative of the B-Spline is larger than 0 along the entire curve. There are some artificial classes of B-Spline curves that do not satisfy this requirement. An example of such a class is the class of B-Splines that has multiple consecutive control points at the same coordinates. But in our field of application this requirement on the derivative will almost surely be met.

### 7.1.1 Construction Scheme

The general control point scheme that we use to construct a single bend curve is shown in Figure 7 below. The order of the control points is the logical order along the curve.

The red control points $\mathbf{E}_1 = \mathbf{P}_6$ and $\mathbf{E}_2 = \mathbf{P}_{12}$ are the given endpoints of the bend curve. So the actual bend we are going to use is the piece of curve between $\mathbf{E}_1$ and $\mathbf{E}_2$. The rest of the control points, and curve, are employed only to make the scheme behave like we need it to.

The lines $L_1$ and $L_2$ are the continuation of the line segments the two endpoints are on.

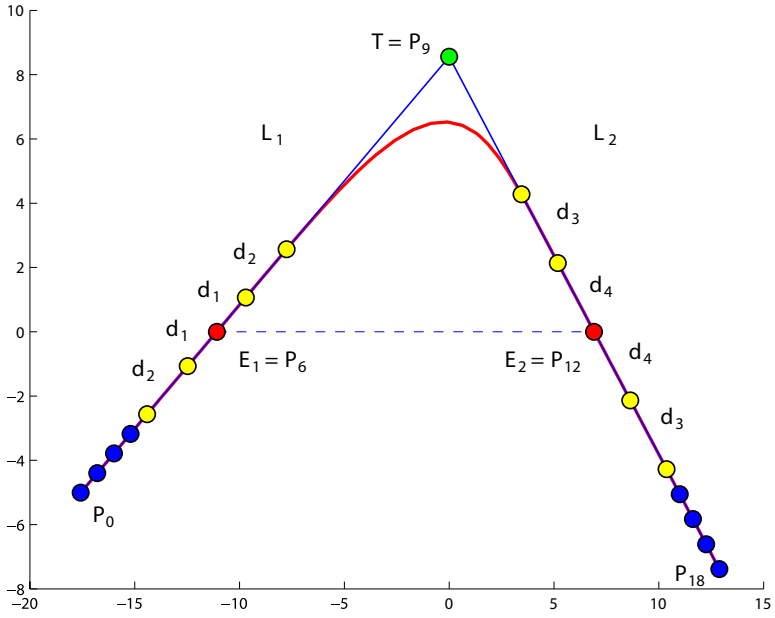


Figure 7: Single Corner Construction

The position of the endpoints $\mathbf{P}_6$ and $\mathbf{P}_{12}$ is given, and should therefore remain fixed. The yellow intermediate points $\mathbf{P}_4$, $\mathbf{P}_5$, $\mathbf{P}_7$ and $\mathbf{P}_8$ have to be located on $L_1$, symmetrical around the endpoint $\mathbf{P}_6$. The yellow intermediate points $\mathbf{P}_{10}$, $\mathbf{P}_{11}$, $\mathbf{P}_{13}$ and $\mathbf{P}_{14}$ need to be positioned on $L_2$, around $\mathbf{P}_{12}$ in the same way. The green top point $\mathbf{T}$ and the blue auxiliary control points can be placed freely.

To show that the control point scheme accomplishes our goal independent of the placement of the top point $\mathbf{T}$ and the auxiliary points, we first need to understand the basis functions involved. Figure 8 shows the basis functions corresponding to the control points in the same colour coding that we used in Figure 7. The names of some important control points are shown above the basis function with which they are multiplied.

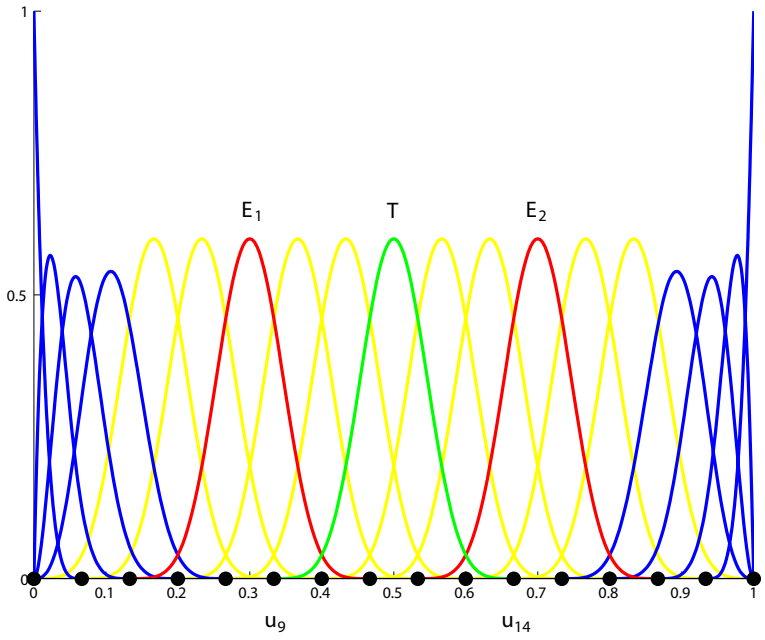


Figure 8: Single Corner Construction

We start by showing that the curve indeed goes through the endpoints $\mathbf{E}_1$ and $\mathbf{E}_2$, i.e., we prove that there are parameter values $e_1, e_2 \in [0,1]$ such that $\mathbf{C}(e_1) = \mathbf{E}_1$ and $\mathbf{C}(e_2) = \mathbf{E}_2$.

**Theorem 7.1.** *Using the control point configuration in Figure 7 we have*

$$\mathbf{C}(e_1) = \mathbf{E}_1 \quad \textit{for} \quad e_1 = \frac{(u_8 + u_9)}{2},$$

*and*

$$\mathbf{C}(e_2) = \mathbf{E}_2 \quad \textit{for} \quad e_2 = \frac{(u_{14} + u_{15})}{2}.$$

*Proof.* We proof the statement for $e_1$ only. The proof for $e_2$ can be conducted using the same method.

The bend curve is given by the B-Spline formulation

$$\mathbf{C}(u) = \sum_{i=0}^{n} \mathbf{P}_i N_{i,4}(u).$$

From Figure 7 we know that $\mathbf{E}_1 = \mathbf{P}_6$. Now define the vectors

$$\mathbf{D}_1 = \mathbf{E}_1 - \mathbf{P}_5 = \mathbf{P}_7 - \mathbf{E}_1,$$

and

$$\mathbf{D}_2 = \mathbf{E}_1 - \mathbf{P}_4 = \mathbf{P}_8 - \mathbf{E}_1.$$

Then, for any $u \in (u_8, u_9)$ we have

$$\begin{aligned}
\mathbf{C}(u) &= \sum_{i=0}^{n} \mathbf{P}_i N_{i,4}(u) = \sum_{i=4}^{8} \mathbf{P}_i N_{i,4}(u) \\
&= (\mathbf{E}_1 - \mathbf{D}_2) N_{4,4}(u) + (\mathbf{E}_1 - \mathbf{D}_1) N_{5,4}(u) + \\
&\quad + \mathbf{E}_1 N_{6,4}(u) + (\mathbf{E}_1 + \mathbf{D}_1) N_{7,4}(u) + (\mathbf{E}_1 + \mathbf{D}_2) N_{8,4}(u) \\
&= \sum_{i=4}^{8} \mathbf{E}_1 N_{i,4}(u) - \mathbf{D}_2 N_{4,4}(u) - \mathbf{D}_1 N_{5,4}(u) + \\
&\quad + \mathbf{D}_1 N_{7,4}(u) + \mathbf{D}_2 N_{8,4}(u) \\
&= \mathbf{E}_1 - \mathbf{D}_2 N_{4,4}(u) - \mathbf{D}_1 N_{5,4}(u) + \mathbf{D}_1 N_{7,4}(u) + \mathbf{D}_2 N_{8,4}(u).
\end{aligned}$$

In the last step we used the fact that

$$\sum_{i=4}^{8} \mathbf{E}_1 N_{i,4}(u) = \mathbf{E}_1 \sum_{i=4}^{8} N_{i,4}(u) = \mathbf{E}_1 \sum_{i=0}^{n} N_{i,4}(u) = \mathbf{E}_1.$$

Since we are using a uniform knot vector we have

$$N_{4,4}\left(\frac{u_8 + u_9}{2}\right) = N_{8,4}\left(\frac{u_8 + u_9}{2}\right),$$

and

$$N_{5,4}\left(\frac{u_8 + u_9}{2}\right) = N_{7,4}\left(\frac{u_8 + u_9}{2}\right).$$

Therefore the above expression for $\mathbf{C}(u)$ gives

$$\mathbf{C}\left(\frac{u_8 + u_9}{2}\right) = \mathbf{E}_1.$$

□

Note that the only control points we used in the above proof are the red endpoints $\mathbf{E}_1$ and $\mathbf{E}_2$, and the yellow intermediate points. Thus Theorem 7.1 is independent of the position of the green top point $\mathbf{T}$ and the blue points. Further note that for this proof we do need the knot vector to be uniform.

A direct consequence of Theorem 7.1 is that the position of the blue auxiliary points does not influence the bend curve. For, as can be seen from Figure 8, the blue basis functions that are multiplied with these control points, are all situated entirely outside the parameter interval $[e_1, e_2]$. We do need the auxiliary points though, as is explained in Section 7.2.

The next step is to show that, at each of the endpoints, the curve is straight and has the same direction as the line segment that endpoint is on. This is actually fairly simple. We show it here for the endpoint $\mathbf{E}_1$ only. The proof for $\mathbf{E}_2$ can be conducted in the same way.

Suppose all control points $\mathbf{P}_1, \ldots, \mathbf{P}_{18}$ would be positioned on the line $L_1$. Then the resulting B-Spline curve is a straight line. As can be seen from Figure 8, at the parameter interval $u \in (u_8, u_9)$ the B-Spline curve is only influenced by the control points $\mathbf{P}_4$,...,$\mathbf{P}_8$. And, according to Theorem 7.1, the endpoint $\mathbf{E}_1$ is attained in the middle of this parameter interval. So if we change the position of the other control points according to the scheme in Figure 7, around $\mathbf{E}_1$ the curve will remain straight and will have the same direction as $L_1$.

### 7.1.2 Top point Positioning

In this section we look at various options for the position of the top point in the control point scheme as shown in Figure 7. We consider four options with plots of the resulting curves.

The control point scheme we use to demonstrate the influence of the position of the top point is the following. The endpoints are given by $\mathbf{E}_1 = (-9, 0)$ and $\mathbf{E}_2 = (9, 0)$. $L_1$ is the line through $\mathbf{E}_1$ and $\mathbf{S}$, and $L_2$ is the line through $\mathbf{E}_2$ and $\mathbf{S}$, where $\mathbf{S}$ is such that $||\mathbf{S} - \mathbf{E}_1||_2 = ||\mathbf{S} - \mathbf{E}_2||_2 = 12$. The position of the yellow intermediate points is determined by $d_1 = d_2 = d_3 = d_4 = 3$.

As shown before, in Section 7.1.1, the position of the blue auxiliary control points does not influence the bend curve. In our examples we have put them very close to the nearest yellow control point, such that they do not show in the plots.

With our control points scheme fixed, we can now examine different positions of the top point $\mathbf{T}$. We only move $\mathbf{T}$ along the angle bisector of the top angle $\angle\,\mathbf{E}_1\mathbf{S}\,\mathbf{E}_2$. Other directions of movement are of course also possible, but lead to similar results.

Each position of the top point we consider is accompanied by three plots. The top plot shows the control points scheme and the resulting bend curve. The middle plot displays the curvature of the curve and the upper and lower bounds on the curvature, as imposed by the steering angle restriction. And the bottom plot shows the first derivative of the curvature with upper and lower bound functions, as imposed by the steering angular velocity restriction. The bounds on the curvature and its derivative are calculated using the vehicle parameters

$$W = 2\,,\ \phi_{\max} = -\phi_{\min} = \pi/4\,,\ \omega_{\max} = -\omega_{\min} = 2\,,\ v_{\min} = 3\,.$$

The first option we look at is placing the top point above the point **S**, see Figure 9. It is clear that the resulting curve is not a single bend any more. Starting in lower left it first bends to the left a bit, then there is a big bend to the right, and finally it bends back to the left a bit again. These are not the kind of curves we are aiming at to construct. If we want to make a curve with multiple bends we should build it from multiple single bend curves.

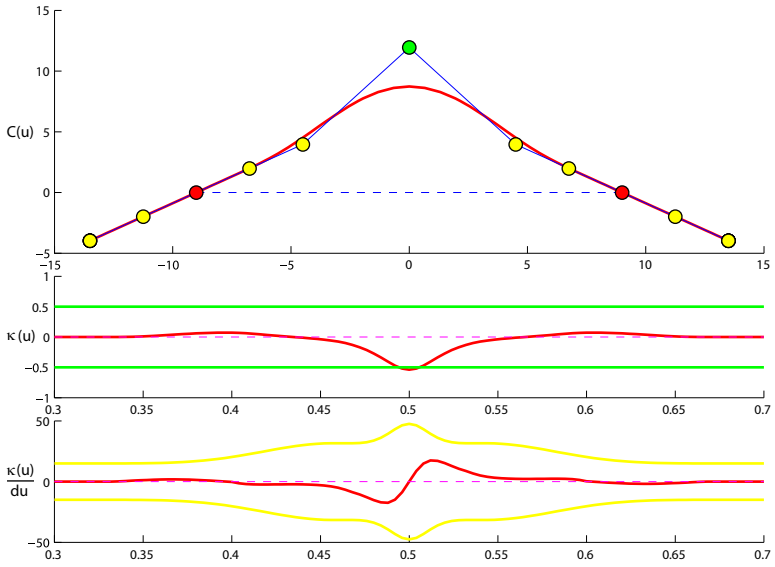


Figure 9: Top point Position 1

The same argument holds when we put the top point very low, as can be seen from Figure 10.

Both the top point positions from Figure 9 and 10 could also be said to be taking a detour. If we interpret the curve as a path to take a certain corner as it was originally intended, then both options take a detour making the path longer than it has to be, with more steering action needed to drive the path. Thus these paths are not efficient.

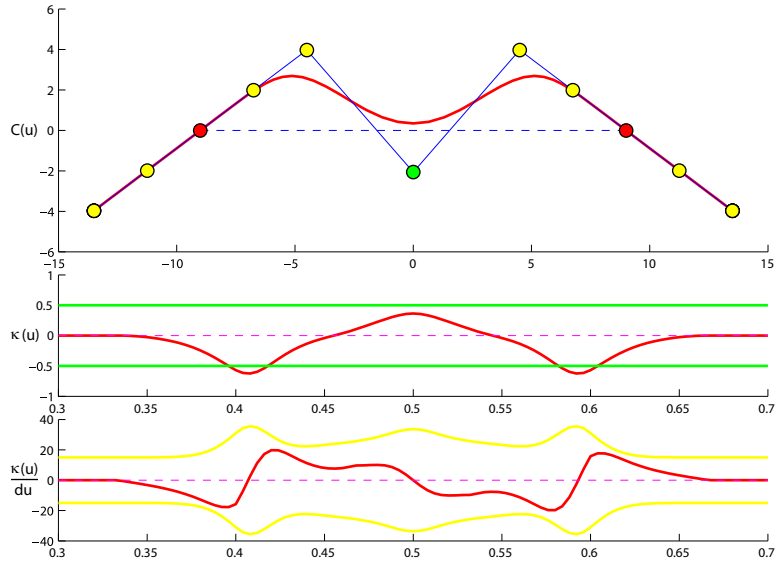


Figure 10: Top point Position 2

There is an interval for the top point, along the angle bisector of the top angle, that results in a bend that does not take a detour. This interval runs from the position $\mathbf{S}$ down to the position $\mathbf{S}'$, where $\mathbf{S}'$ is the position that results in a curve that has a curvature of 0 at $\mathbf{C}(0.5)$. The options $\mathbf{S}$ and $\mathbf{S}'$ are shown in Figure 11 and Figure 12 respectively.

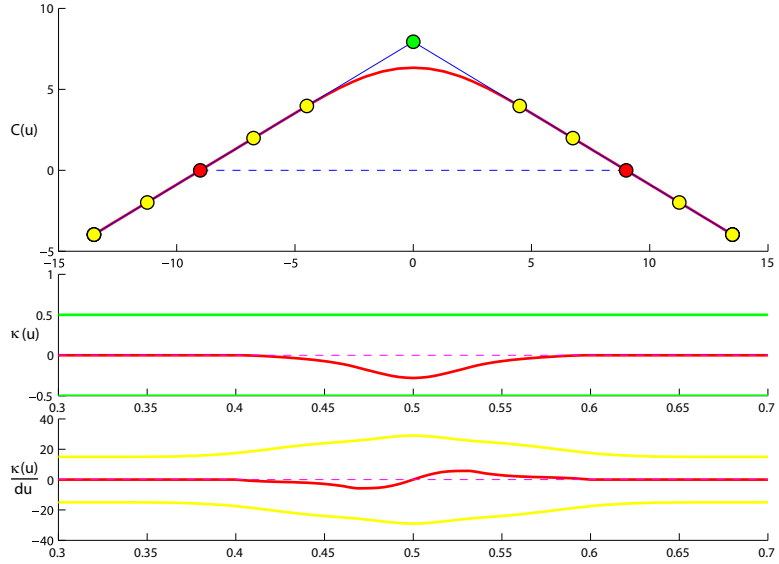


Figure 11: Top point Position 3

In terms of vehicle control, putting the top point at position **S** corresponds to steering into the corner and back as smoothly as is possible within the bounds of our configuration scheme. It results in a smooth curve with only a single bend, that puts as little strain as possible on the vehicle and its contents. This is obviously a very natural choice for the top point position.

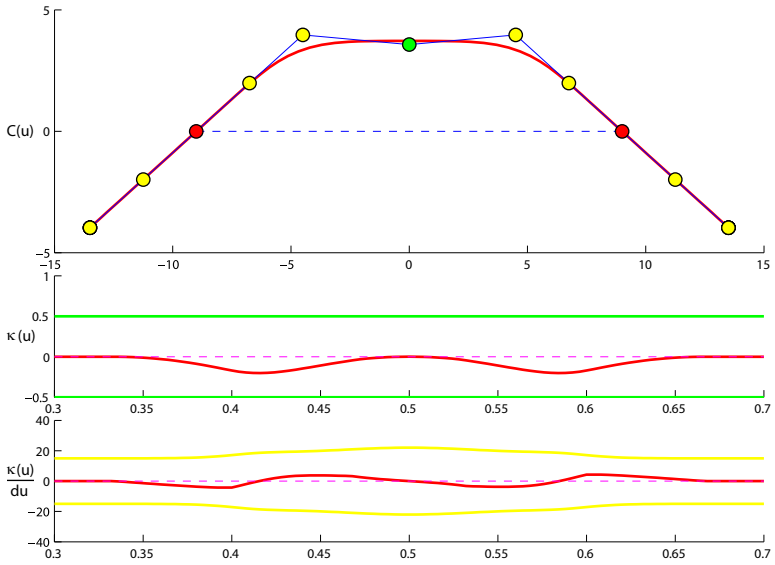


Figure 12: Top point Position 4

Positioning the top point at $\mathbf{S}'$ corresponds to steering into the corner as fast as possible, then steering back and going straight for a while in the middle of the curve, then steering as fast as possible again to complete the corner. This bend is not as smooth as the previous one, and puts more strain on the vehicle and its contents. But, depending on the steering motor and mechanism it might possibly be more power efficient, because there is a small part in the middle of the bend where no steering action is required.

However, again, if we want a curve like this we could build it from two smooth single bends. Therefore we will use **S** as the default position for the green top point.

Now that we have chosen a fixed position of our top point, it could be argued that we do not need this top point any more. We could leave it out and let the yellow control points $\mathbf{P}_8$ and $\mathbf{P}_{10}$ coincide into a new fixed top point. All essential properties of the control point configuration scheme would remain. This would greatly reduce the flexibility in shaping the curve, however, as well as reducing our flexibility when connecting single bend curves to form a larger curve with multiple bends. Therefore we have chosen to keep the top point, to retain the flexibility of our control point scheme.

### 7.1.3 Intermediate Point Positioning

In the previous sections we introduced a control point scheme for the construction of a bend curve, showed that the blue auxiliary control points do not influence the shape of this bend curve, and argumented that we will usually keep the green top point at a fixed position. This leaves the yellow intermediate points as parameters to shape the bend curve.

In Appendix A we present plots of several distinct choices for the placement of the intermediate points. We use these plots to describe the influence the placement of those points has on the shape of the curve.

In each of the plots the knots of the B-Spline curve are marked. The placement of the shaping points has a strong influence on the position of the knots, in relation to the control point scheme. Since we plotted each knot $u_i$ as a marker at $\mathbf{C}(u_i)$ in the plot of the bend curve, we conveniently interchange the notions of a knot value and the value of the curve at that knot.

We saw in Theorem 7.1 already that the endpoint $\mathbf{E}_1$ lies between the knots $u_8$ and $u_9$. Also, from Figure 8 we can see that the position of the top point $\mathbf{T} = \mathbf{P}_9$ only influences the curve between $u_9$ and $u_{14}$. However we chose to keep the top point at a fixed position, at the intersection of the lines $L_1$ and $L_2$. In the same way, the position of $\mathbf{P}_8$ only influences the curve between $u_8$ and $u_{13}$, and the position of $\mathbf{P}_{10}$ only influences the curve between $u_{10}$ and $u_{15}$.

Following the same argumentation we used in Section 7.1.1 to show that the bend curve is straight around the endpoints, we can now conclude that the bend curve is straight along $L_1$ from $\mathbf{E}_1$ to $u_{10}$, and straight along $L_2$ from $u_{13}$ to $\mathbf{E}_2$. Thus, only the part of the curve between $u_{10}$ and $u_{13}$ is rounded.

Since the original idea was to make a rounded curve between two given endpoints, it makes sense to choose the positions of the intermediate points in such a way that $u_{10}$ is close to the endpoint $\mathbf{E}_1$, and that $u_{13}$ is close to the endpoint $\mathbf{E}_2$. From the plots in Appendix A it can be seen that $u_{10}$ is approximately halfway between $\mathbf{P}_7$ and $\mathbf{P}_8$ in most cases, except when both of those points are either very close to the endpoint $\mathbf{E}_1$, or very close to the top point. But even then $u_{10}$ is close to the point halfway $\mathbf{P}_7$ and $\mathbf{P}_8$, relative to the larger scale of the entire bend curve.

From the above observations we derive the following rule of thumb, that can be used to ensure there will not be a large piece of straight curve around the endpoints:

*The intermediate points $\mathbf{P}_7$ and $\mathbf{P}_8$ should be placed close to the endpoint $\mathbf{E}_1$, and the intermediate points $\mathbf{P}_{10}$ and $\mathbf{P}_{11}$ should be placed close to $\mathbf{E}_2$.*

Note that the position of the intermediate points $\mathbf{P}_4$, $\mathbf{P}_5$, $\mathbf{P}_{13}$ and $\mathbf{P}_{14}$ is also determined by this rule, since they are linked to the other intermediate points.

An example of a curve resulting from the above rule of thumb, is shown in Figure 13. In this figure we used the same control point scheme as in Appendix A.

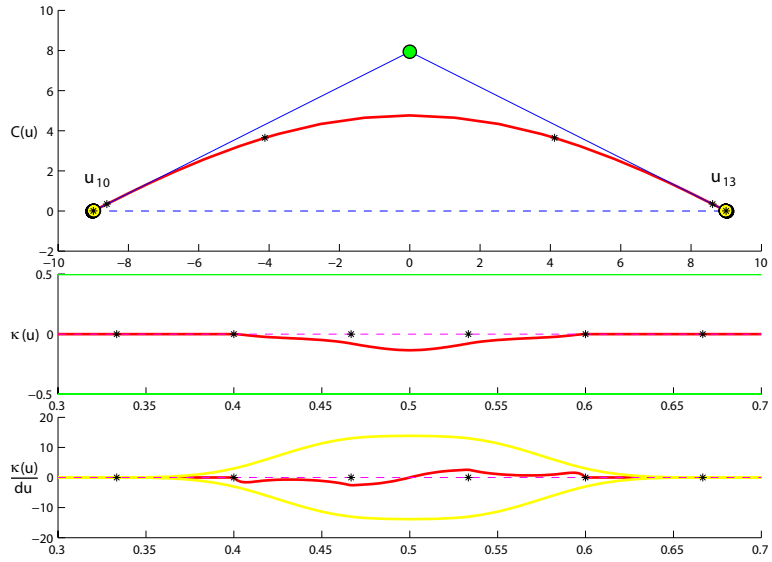


Figure 13: Curve Shaping: $d'_1 = d'_2 = d'_3 = d'_4 = 1/1000$

An additional advantage of placing the yellow intermediate points close to the endpoints, is that our control point scheme does not have to extend far outside $\triangle \mathbf{E}_1\mathbf{T}\mathbf{E}_2$, unlike for example the scheme shown in Figure 22. As is discussed in Section 7.2, this is very convenient when connecting single bend curves to form a larger path.

## 7.2 Connecting Single Bend Curves

In the previous section we explained how to design single bend curves. The next step is to connect such curves, to create a larger path curve. We show how to connect two single bend curves $A$ and $B$, using a superscript $A$ or $B$ on curve parameters to indicate to which curve they belong.

To connect two single bend curves $A$ and $B$ and merge them into a single larger path curve, we have to make one end of curve $A$ the same as one end of curve $B$. Only then we can overlap these ends and merge the two curves into one.

When we overlap two control points of two different curves to merge them, we obviously can only have one basis function belonging to that control point in the merged curve. Therefore, if the control points had basis functions with different shapes belonging to them, merging them could change the shape of one of the original single bend curves, because at least one of the control points will by multiplied by a different basis function in the merged curve.

This is why, in the construction scheme introduced in Section 7.1.1, we have used four blue auxiliary control points on each side of the scheme. These points, together with the fact that we are using a uniform knot vector, ensure that all basis functions that influence the actual bend curve between the endpoints have the same shape.

With this knowledge it is now fairly simple to connect two single bend curves. For the merged curve we again use a uniform knot vector, but with more knots. This way all basis functions for the merged curve, have the same shape as the basis functions for the two original bend curves.

The only exceptions are the basis functions that belong to those four auxiliary points of each of the curves that overlap with the other curve. The basis functions belonging to these points are different in the merged curve. However, this does not pose a problem since the auxiliary points do not influence the actual bend curves.

Figure 14 below illustrates how to connect the curves $A$ and $B$, if we want a straight piece of curve with length $q$ between the two curves, where

$$q = \left|\left|\mathbf{E}_2^A - \mathbf{E}_1^B\right|\right|_2 = d_1^B + d_2^B + d_3^A + d_4^A + \bar{q}\ , \quad \text{with } \bar{q} > 0.$$

Since we are free to place the blue auxiliary points of either curve wherever we like, we can set

$$\mathbf{P}_{15}^A = \mathbf{P}_4^B\ , \quad \mathbf{P}_{16}^A = \mathbf{P}_5^B\ , \quad \mathbf{P}_{17}^A = \mathbf{P}_6^B\ , \quad \mathbf{P}_{18}^A = \mathbf{P}_7^B\ ,$$

and

$$\mathbf{P}_0^B = \mathbf{P}_{11}^A\ , \quad \mathbf{P}_1^B = \mathbf{P}_{12}^A\ , \quad \mathbf{P}_2^B = \mathbf{P}_{13}^A\ , \quad \mathbf{P}_3^B = \mathbf{P}_{14}^A\ ,$$

to accomplish the connection shown in Figure 14.

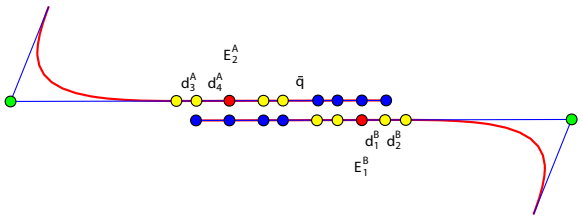


Figure 14: Connecting Bend Curves 1

If we do not want a straight piece between the endpoints, we can connect the curves $A$ and $B$ as shown in Figure 15. In this type of connection we set

$$\mathbf{E}_2^A = \mathbf{E}_1^B \,,$$

and set the surrounding control points to overlap too, as shown in Figure 15. Note that the blue auxiliary points are not shown in the correct position, because this would unnecessarily complicate the image. Each should be placed overlapping the next control point in line, like in Figure 14.

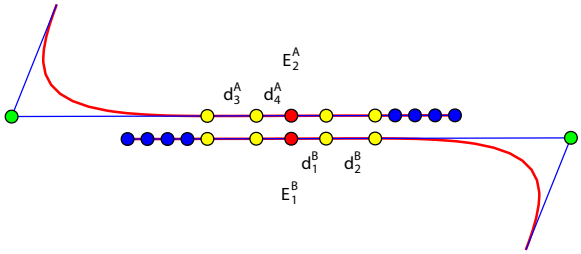


Figure 15: Connecting Bend Curves 2

A direct consequence of this type of connection is that we need to set

$$d_1^B = d_4^A \quad \text{and} \quad d_2^B = d_3^A \,.$$

If we want a straight piece with length $q \leq d_1^B + d_2^B + d_3^A + d_4^A$ between the endpoints, a connection type could be used that lies somewhere between the two extreme options we have shown. However, as we saw in Section 7.1.3, we usually want to place the yellow shaping points very close to the endpoints. As a result $q$ will be very small, and we will have no need for any of the intermediate connection types.

## 7.3 Feasibility

As for any path, when we construct a path from single bend curves, we want the path to be feasible, i.e., we want the vehicle for which we are designing the path to be able to drive that path. In previous sections we have already developed tools for this purpose. In this section we discuss how they can be used when constructing a path from single bend curves.

Since vehicles that cannot drive straight usually do not make much sense, we assume the vehicle can. Therefore all straight pieces between curves are always feasible, and we can restrict ourselves to checking the feasibility of each single bend curve. If all curves from a set of single bend curves are feasible for a certain vehicle, that vehicle will be able to drive any path composed of these bend curves.

It is not hard to check the feasibility of a single bend curve. We can discretize the interval of the curve parameter $u$, and use equations (3) and (8), to test if the curve is feasible at the discretized parameter values.

The problem becomes more difficult if we want to calculate how we can reposition the control points in the construction scheme to get a feasible curve. However, all important operations on the configuration scheme can be described as the repositioning of one or more control points along a single line. Therefore we can use the method to calculate the feasible repositioning interval, developed in Section 5, with the extension treated in Section 6.2 if needed.

If we want to reposition the top point along the angle bisector of the top angle, we can directly use the theory developed in Section 5. If we want to reposition an intermediate point, then another intermediate point moves with it in opposite direction. This can easily be described as a multiple control point repositioning, by setting $\boldsymbol{\alpha}$ to the direction of movement, and setting the $\zeta_i$ values to $+1$ and $-1$ respectively for the two moving intermediate points, and to 0 for all other control points.

As we explained in Section 7.1.2 and 7.1.3, the repositioning of the top point and intermediate points is not needed in most cases. Usually the curve is determined by the choice of the position of the endpoints, with the neighbouring intermediate points close to it. Changing the position of an endpoint along a line, can also be described as a multiple control point repositioning. We can do this by setting the $\zeta_i$ values for the endpoint we want to move and its four neighbouring intermediate points all to 1, and to 0 for all other control points.

An interesting note is, that these repositioning principles can still be directly applied on single bend curves after they have been merged into a larger path curve.

## 7.4 Variations and Alternatives

There are a lot of possible variations on the construction concept we have presented in the foregoing sections. There are also interesting, altogether different options to construct path curves. In this section we will describe some of these variations and alternatives.

As explained in Section 7.1.2, we can simplify the construction scheme by removing the green top point. The opposite is also a possibility. We could insert more control points between the top point and the neighbouring intermediate points. These points could be placed freely, and would dramatically increase the flexibility of shaping single bend curves.

In our construction method we have only treated the use of B-Spline single bend curves, created by means of our control point scheme, and straight lines. A very good addition would be to introduce more standard shapes to combine with the curves. By far the most interesting additional shape is a circular bend, because a vehicle that complies with the vehicle model presented in Section 3.1 can follow a circular bend by keeping one fixed steering position along the entire bend. For the steering installation, this is the most energy efficient way possible to take a corner.

An entirely different approach would be to try to construct the entire path from one single curve, instead of construction parts and connecting them. To do this, we would have to start with some approximation of the path the vehicle has to drive. Since B-Spline and NURBS theory offers some nice interpolation and approximation tools, see [PT97], we could get a set of points along the desired path and interpolate or approximate a curve through it.

After inserting control points to get a good spread and density of control points on the initial approximation of the path, we could change the positions of the control points in order to create a better path for the vehicle. This could be done by hand or, preferably, by some optimization algorithm.

# 8 Conclusions and Recommendations

The ultimate goal of FROG Navigation Systems, the company that initiated this research project, is to develop a tool that can automatically generate the optimal vehicle path for a certain vehicle given a map of the area and a starting point and destination.

This is a very ambitious goal and we are still far away from it. However, the methods developed in this report are big steps in the right direction. In this final section we discuss the value of our research for FROG, and make recommendations on how to proceed to that ambitious goal.

The most important merit of our research is the work on feasible repositioning sets for B-Spline paths. With it the internal constraint problem mentioned in Section 1, is effectively solved. These constraints were the biggest problem for human designers who had to construct a path manually, which makes our method to calculated feasible repositioning sets invaluable on its own.

So far only small tests have been run, calculating the feasible repositioning sets of small curves with a MATLAB implementation of the developed methods. All tests conducted within parameters anywhere near the FROG application behaved very nicely. Since the calculation of the feasible repositioning set is a local problem, there is no reason that the application on full scale practical problems would give any trouble.

The fact that we reposition a control point along a line is not really a limitation. In most cases it is preferred to move a control point at right angles to the curve at that point. And otherwise it is easy to combine the feasible repositioning sets along different lines into an approximated feasible repositioning area for a control point.

In Section 6.1 we extended the repositioning principle from B-Splines to NURBS curves. There are more options when working with NURBS curves though. The difference between NURBS and B-Splines is the set of weights that NURBS curves use. If we want to use the extra flexibility that NURBS curves get from these weights, we should allow not only control point repositionings, but also weight changes.

Further it should be noted that the developed calculation method for feasible repositioning sets is only usable for the vehicle model presented in Section 3.1. However, almost all FROG vehicles can be modeled by the presented model.

The feasible repositioning sets find a nice application in the path construction method presented in Section 7. This construction method is not universally applicable. It is not very suitable for the construction of paths along

the winding roads we usually find in everyday traffic. But it is very good for industrial applications where the road system is less complex, which is currently the main field of application for FROG.

The presented construction method was developed from a principle used by FROG. The designer would manually add the intermediate points that lie between the two endpoints, and the top point. We put this into a control point scheme to make sure that the positions would be correct, and to take the work out of the hands of the designer. Further we added the control points outside the endpoints to be able to merge curves together without complications. Finally we researched the scheme to find the best values for its parameters.

Summarizing, we developed the following tools for B-Spline paths:

- A solution of the internal constraint problem through the calculation of feasible repositioning sets.
- A user friendly path construction method for industrial applications that can use feasible repositioning sets to construct a feasible path.

Constructing vehicle paths by hand is an enourmous task, and very time consuming. The developed tools can reduce the time to produce feasible vehicle paths greatly.

The most interesting directions for further research are:

- Complement the method to calculate feasible repositioning sets, with a method to calculate feasible intervals for weights in NURBS curves.
- Extend the path construction method with some of the options mentioned in Section 7.4.
- Develop tools to solve the external constraint problem.

The first two of these research directions are further developments of the research we have done. When completed they make the methods we developed in this report even more flexible.

The development of a solution to the external constraint problem is the next big step in the direction of the ultimate goal. From here we can continue by quantifying what is a good feasible path, and what is a bad one, and finally combine the results together with our internal constraint research into a solver algorithm that automatically constructs a good path.

# A Single Bend Curve Shaping

This section shows plots of the resulting curve when we use the yellow shaping points in the control point scheme, introduced in Section 7.1.1, to shape the curve.

The control point scheme we use is the following. The endpoints are given by $\mathbf{E}_1 = (-9, 0)$ and $\mathbf{E}_2 = (9, 0)$. $L_1$ is the line through $\mathbf{E}_1$ and $\mathbf{S}$, and $L_2$ is the line through $\mathbf{E}_2$ and $\mathbf{S}$, where $\mathbf{S}$ is such that $||\mathbf{S} - \mathbf{E}_1||_2 = ||\mathbf{S} - \mathbf{E}_2||_2 = 12$.

Let $d_1'$ and $d_2'$ denote the fractions $d_1$ and $d_2$ are of $||\mathbf{S} - \mathbf{E}_1||_2$, and let $d_3'$ and $d_4'$ denote the fractions $d_3$ and $d_4$ are of $||\mathbf{S} - \mathbf{E}_2||_2$, i.e., $d_i' = d_i/12$ for $i = 1, \ldots, 4$. As a reference we use $d_3' = d_4' = 1/4$ in all plots. The values $d_1'$ and $d_2'$ are varied to show how the position of the shaping points influences the shape of curve.

Each choice for the positions of the shaping points is accompanied by three plots. The top plot shows the control points scheme and the resulting bend curve. The middle plot displays the curvature of the curve with upper and lower bounds. And the bottom plot shows the first derivative of the curvature with upper and lower bound functions. The bounds on the curvature and its derivative are calculated using the vehicle parameters

$$W = 2\,,\ \phi_{\max} = -\phi_{\min} = \pi/4\,,\ \omega_{\max} = -\omega_{\min} = 2\,,\ v_{\min} = 10\,.$$

Black asterisks are used to indicate the position of knots in the plots.

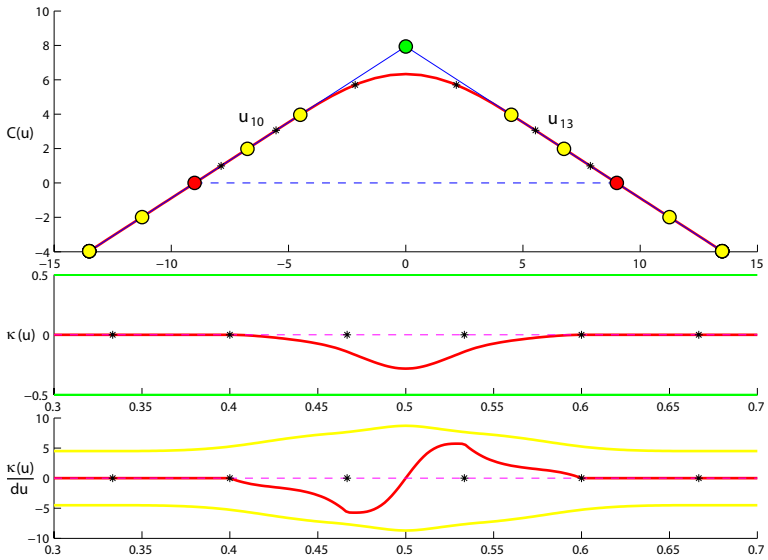


Figure 16: Curve Shaping: $d_1' = 1/4$, $d_2' = 1/4$

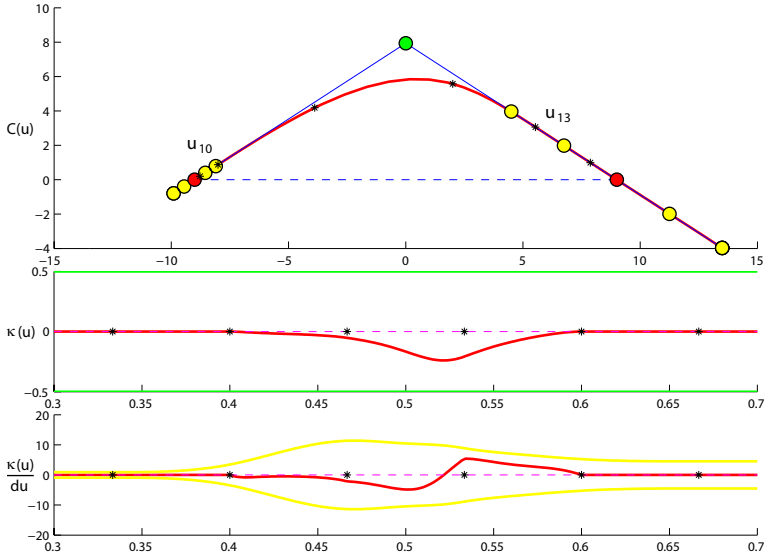


Figure 17: Curve Shaping: $d'_1 = 1/20$, $d'_2 = 1/20$

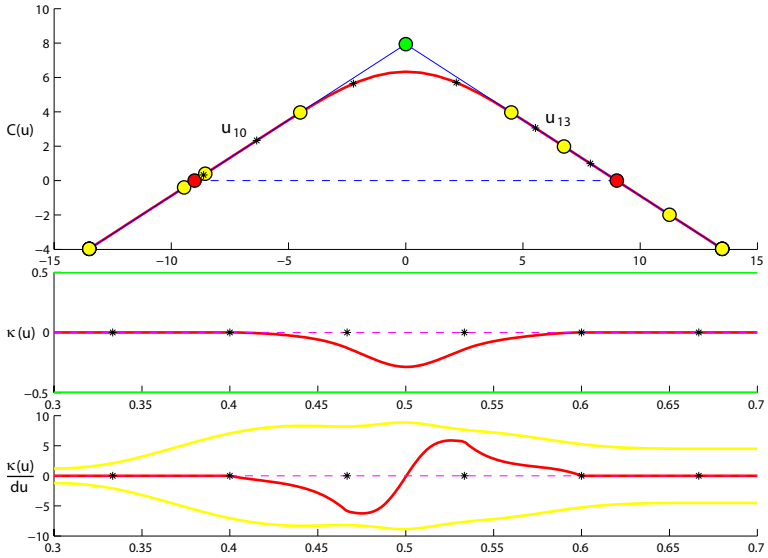


Figure 18: Curve Shaping: $d'_1 = 1/20$, $d'_2 = 9/20$

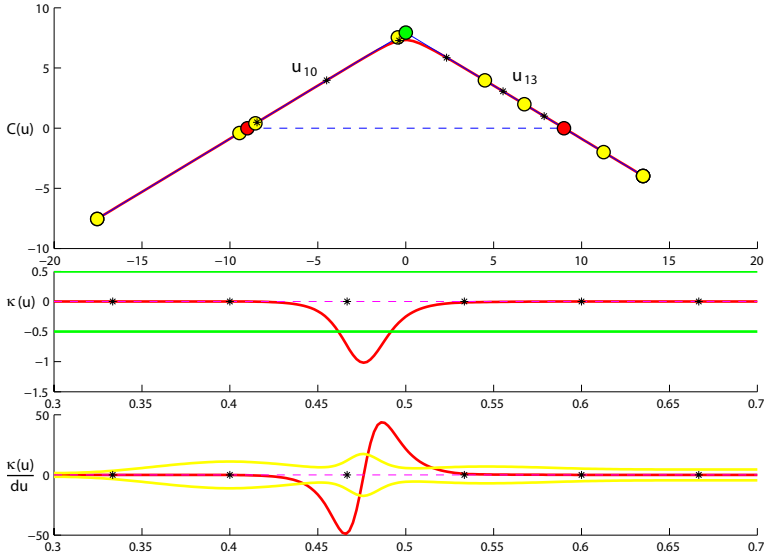


Figure 19: Curve Shaping: $d'_1 = 1/20$, $d'_2 = 18/20$

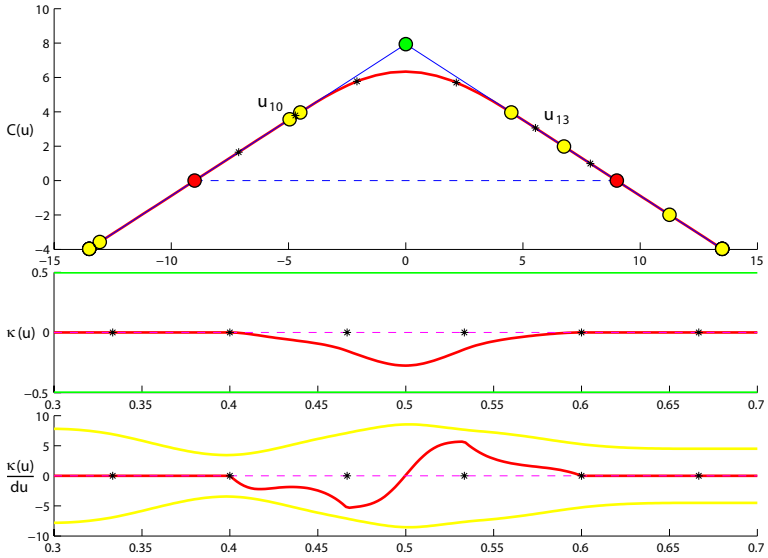


Figure 20: Curve Shaping: $d'_1 = 9/20$, $d'_2 = 1/20$

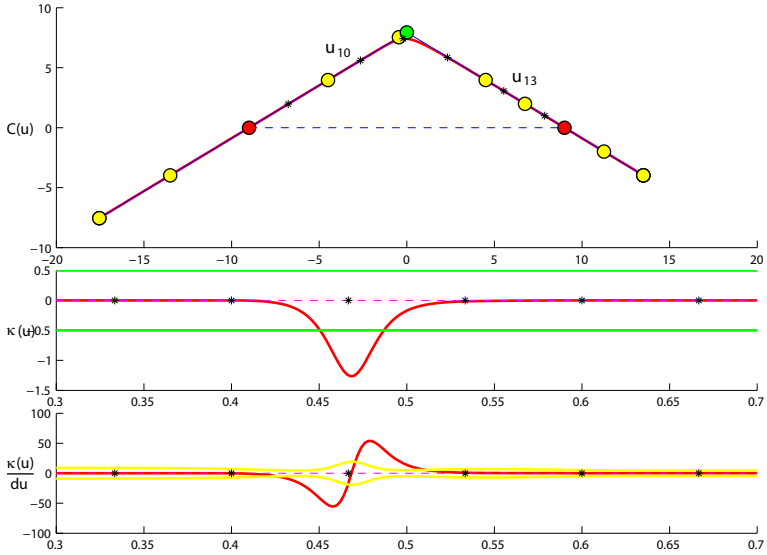


Figure 21: Curve Shaping: $d'_1 = 1/2$, $d'_2 = 9/20$

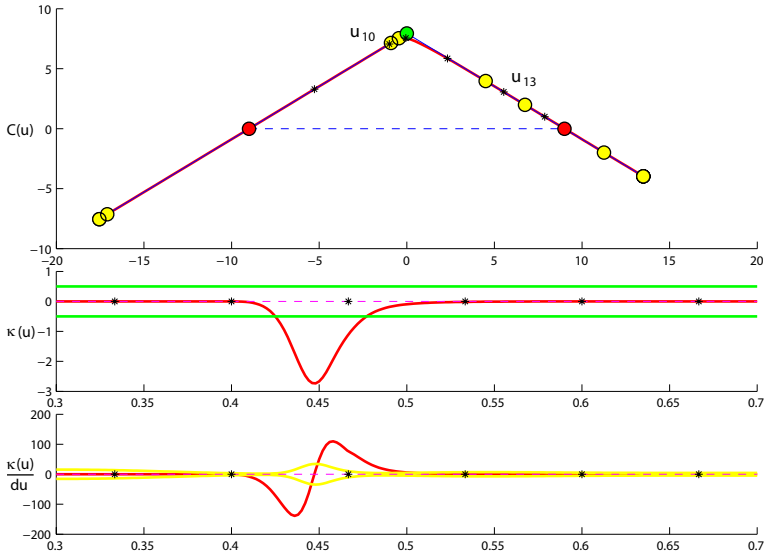


Figure 22: Curve Shaping: $d'_1 = 18/10$, $d'_2 = 1/20$

# References

[dB01] Carl de Boor. *A Practical Guide to Splines*. Springer-Verlag, New York, revised edition, 2001.

[Ide05] Reijer Idema. Optimal path synthesis for automated guided vehicles: Preliminary research. Master's thesis, Delft University of Technology, 2005.

[PT97] Les Piegl and Wayne Tiller. *The NURBS Book*. Springer-Verlag, Berlin, second edition, 1997.